"Enhanced Wellbore Stabilization and Reservoir Productivity with Aphron Drilling Fluid Technology"

QUARTERLY PROGRESS REPORT

January 1 – March 31, 2005

by

Fred Growcock

Issued April, 2005

DOE Award Number DE-FC26-03NT42000

MASI Technologies *LLC*
8275 El Rio Street, Suite 130
Houston, Texas 77054

DISCLAIMER

ABSTRACT

The task areas for Phase II include Aphron Drilling Fluid Optimization, Flow Properties and Leak-Off and Formation Damage in Permeable Media. During Q2, optimization efforts of the current APHRON ICS™ formulation suggest that increased bubble stability may result from reducing the concentration of viscosifier and increasing the concentration of plasticizer. Aphron generation through expansion in nozzles was simulated with some pressure drop tests through an orifice at elevated pressure; however, for an APHRON ICS™ fluid containing dissolved air equivalent to the typical amount of air incorporated in that fluid, no aphrons were observed. Contact angle measurements of APHRON ICS™ mud on glass pre-wetted with a couple of crude oils showed that the mud will spread and that the fluids are compatible.

In the area of Flow Properties, viscosity profiles of APHRON ICS™ muds containing various amounts of air indicate that, above 10 to 15 vol % air, the viscosity increases for shear rates above 1 rpm (1.6 sec^{-1}), but not below that shear rate. The effect of temperature over the range 76 to 150 ^{o}F is quite modest; only above 100 rpm (160 sec^{-1}) was any reduction in viscosity observed. A fluid invasion model has been developed by Dr. Peter Popov of Texas A&M University, which shows that, under downhole conditions, the rheology of the APHRON ICS™ fluid can limit depth of invasion to a few meters. Additional work will need to be carried out to quantify the effects of other drilling fluid components.

Finally, in the area of Formation Invasion and Damage Potential, linear, static Leak-Off tests at 200 ^{o}F, Fore-Pressure = 2000 psig and Back-Pressure = 1000 psig showed the APHRON ICS™ fluid can seal Aloxite cores ranging in permeability from 2 to 10 Darcy; the Leak-Off is commensurate with the permeability of the core. For comparison, a solids-free standard reservoir drilling fluid was not able to seal even the 2-Darcy core. With addition of 30 ppb $CaCO_3$, both fluids prepared with 10% NaCl provided similar, very low Leak-Off. [To confirm these results under downhole conditions, Leak-Off and Return Permeability tests need to be carried out dynamically in radial geometry with long filter media.] Capillary Flow tests, along with Core Leak-Off and Modified Capillary Suction tests indicate that, in addition to very high low-shear-rate viscosity and aphrons, the solids and surfactants in APHRON ICS™ drilling fluids play major roles in reducing fluid invasion in both low- and high-permeability media.

TABLE OF CONTENTS

LIST OF FIGURES

INTRODUCTION

Aphron drilling fluids have been applied successfully worldwide to drill depleted reservoirs and other high-permeability formations. Aphrons are specially designed air-filled bubbles that are usually incorporated into the fluid with conventional mud mixing equipment, thereby reducing costs and safety concerns associated with air or foam drilling. Because the amount of air in the fluid is very low, the density of the fluid downhole is essentially that of the base fluid. Yet, the fluid is able to seal loss zones effectively and with minimal formation damage. Consequently, aphron drilling fluids are marketed as cost-effective alternatives to underbalanced drilling.[1-4]

Aphron drilling fluids possess two chief attributes that serve to minimize fluid invasion and damage to the formation. First, the base fluid is very shear-thinning and exhibits an extraordinarily high LSRV (Low-Shear-Rate Viscosity); this high viscosity is thought to reduce the flow rate of the fluid dramatically upon entering a loss zone. Second, very tough and flexible microbubbles are incorporated into the bulk fluid with conventional mud mixing equipment. These highly stabilized bubbles, or "aphrons," are considered essential to sealing the problem area and are thought to do so by bridging within the loss zone rather than at its periphery.

Water-based aphrons consist of two essential elements: a spherical core of air and a protective outer shell.[5] In contrast to a conventional air bubble, which is stabilized by a surfactant monolayer, the outer shell of the aphron is thought to consist of a much more robust surfactant tri-layer. This tri-layer is envisioned as consisting of an inner surfactant film enveloped by a viscous water layer, outside of which an outer bilayer of surfactants provides rigidity and low permeability to the structure while imparting some hydrophilic character to it. Under quiescent conditions, the structure is compatible with the aqueous bulk fluid, but it is speculated that the shell is non-ionic, hence has little affinity for charged mineral surfaces (pore walls) or for other aphrons.

It has been claimed that aphrons are a unique type of lost circulation material, forming a micro-environment in a pore network or fracture that appears to behave in some ways like a foam, and in other ways like a solid, but flexible bridging material. As is the case with any bridging mate-

rial, concentration and size of the aphrons are critical to the mud's ability to seal thief zones. Aphrons are created and entrained in the bulk fluid with standard mud mixing equipment, which reduces the safety concerns and costs associated with high-pressure hoses and compressors commonly utilized in air or foam drilling.[6] Although each application is customized to the individual operator's needs, the mud system is generally designed to contain 12-15% by volume air. Aphrons are thought to be sized or polished at the drill bit to achieve a size of 15-100 μm diameter, depending on pressure, which is typical of many bridging materials.

Various aspects of the aphrons, particularly their physicochemical properties, need to be evaluated further to understand the way that they function and to enhance their performance. Greater application of aphron technology and the consequent reduction in drilling costs would be facilitated by a systematic and thorough evaluation of the structure and behavior of aphron drilling fluids under downhole conditions.

The objectives of this project are threefold: (a) develop a comprehensive understanding of how aphrons behave at elevated pressures and temperatures; (b) measure the ability of aphron drilling fluids to seal permeable and fractured formations under simulated downhole conditions; and (c) determine the role played by each component of the drilling fluid.

The Project is divided into two phases. In Phase I (Year 1) the thrust of the work was to develop evidence for the ways in which aphrons behave differently from ordinary surfactant-stabilized bubbles, particularly how they seal permeable and micro-fractured formations during drilling operations.

One key learning of the work conducted during Phase I is that the base fluid is very highly shear-thinning and possesses a low-shear-rate viscosity much higher than conventional reservoir drilling fluids. Furthermore, low thixotropy enables the fluid to generate high viscosity very quickly when entering a loss zone. Second, aphrons can survive substantial downhole pressures for a significant period of time. In a loss zone, this feature may enable the bubbles to migrate faster than the base liquid and concentrate at the fluid front, thereby building an internal seal in the pore network of the rock. Another key learning is that aphrons have very little attraction for each other or for mineral surfaces, as had been hypothesized. Consequently, they do not readily coa-

lesce nor do they stick easily to the pore walls. As a result, aphrons are produced back relatively easily, leaving little permanent formation damage.

Phase II (Year 2) focuses on optimization of the structure of aphrons and composition of aphron drilling fluids, quantifying the flow properties of the fluids (radial vs linear flow, shear and extensional viscosity effects and bubbly flow phenomena), and understanding formation sealing and damage under simulated downhole conditions (including scale-up tests), so as to furnish irrefutable evidence for this technology and provide field-usable data.

The current schedule of tasks is provided in Figure 1.

Figure 1. Schedule of Tasks in Aphron Drilling Fluid Project

	2003	2004				2005		
Task	4th Q	1st Q	2nd Q	3rd Q	4th Q	1st Q	2nd Q	3rd Q
1. Aphron Compressibility								
1.1 Aphron Visualization	X	X	X					
1.2 Fluid Density	X	X	X					
1.3 Aphron Air Diffusivity	X	X	X	X				
2. Sealing Mechanism								
2.1 In Situ Visualization			X	X				
2.2 Pressure Transmissibility	X	X	X					
2.3 Aphron Shell Hydrophobicity			X	X				
3. Leak-Off/Formation Damage - Initial Tests								
3.1 Sealing of Permeable Media			X	X				
3.2 Sealing of Fractured Media			X	X				
4. Aphron Drilling Fluid Optimization								
4.1 Microstructure					X	X		
4.2 Performance					X	X		
5. Flow Properties								
5.1 Geometry of Medium					X	X		
5.2 Fluid Rheology						X		
5.3 Multi-Phase Flow Effects						X		
6. Leak-Off/Formation Damage Perm Media								
6.1 Lab Tests Leak-Off/Return Perm						X		
6.2 Field-Sim Tests Leak-Off/Return Perm								

Phase I ran from Oct. 1, 2003 through Sept. 30, 2004 and consisted of Task Areas 1-3. Phase II runs from Oct. 1, 2004 through Sept. 30, 2005. In Phase II, the main task areas are as follows:

Task Area 4. Aphron Drilling Fluid Optimization - The composition of the polymeric water-based aphron drilling fluid and the method of generating aphrons will be varied to optimize the pressure/temperature stability of the fluid, its ability to reduce leak-off and its ability to be removed with minimal damage to producing formations.

Task Area 5. Flow Properties – The effects of radial geometry of the borehole; aphron concentration; cavitation and extension as well as shear; and multi-phase aspect of the polymeric water-based aphron drilling fluid on its flow behavior in permeable formations will be explored. A fluid invasion model will be developed that takes into account bubbly flow and can be used to predict rate and extent of invasion of aphron drilling fluids. Sub-Task Area 5.3 was begun this last Quarter, several months earlier than originally planned, in order to take advantage of the availability of Dr. Peter Popov, who is developing a fluid invasion model of the APHRON ICS™ system.

Task Area 6. Leak-Off and Formation Damage in Permeable Media – Using results from Task Area 5, Core Leak-Off and Return Permeability measurements will be carried out with both linear and radial flow, static and dynamic flow of the fluid in the "wellbore", and short to very long cores and sand packs. Effects of fore pressure, back pressure, temperature, rate of fluid compression and chemical composition of aphron drilling fluids will also be varied to characterize the Leak-Off behavior of the fluids. Sub-Task Area 6.1 was begun this last Quarter because of the need for some Leak-Off test data for Shell and the importance of obtaining some Capillary Flow Tube data for the fluid invasion model being developed under Task Area 5.

EXECUTIVE SUMMARY

During the Second Quarter of Phase II, work was continued in all three task areas: (a) Aphron Drilling Fluid Optimization - the composition of the polymeric water-based aphron drilling fluid and the method of generating aphrons are varied to optimize the ability of the fluid to reduce leak-off at elevated pressures and temperatures with minimal formation damage; (b) Flow Properties – A fluid invasion model is being developed that incorporates the effects of radial geometry of the borehole, aphron concentration, fluid cavitation and extension as well as shear, and multi-phase flow; and (c) Leak-Off and Formation Damage in Permeable Media –Core Leak-Off and Return Permeability measurements are being carried out at various pressures and temperatures and varying fluid composition using both linear and radial flow, static and dynamic flow of the fluid at the face of the permeable zone, short and long permeable samples and a broad permeability range.

Aphron Drilling Fluid Optimization focused on Chemical Composition and Morphology, Aphron Generation Methodology and Surface Chemistry of Aphron Drilling Fluids. A test matrix of 16 formulations designed to optimize the current APHRON ICS^{TM} formulation has been examined, which appears to show that reducing the concentration of viscosifier and increasing the concentration of plasticizer produces greater bubble stability. However, other properties, such as fluid invasion, need to be examined before recommending any change to the fluid formulation. Aphron formation via expansion through drill bit nozzles was simulated with some pressure drop tests through an orifice. Using an inlet pressure of 2000 psig and an outlet pressure of 1500 psig outlet, it was demonstrated that aphrons cannot be formed under these conditions from APHRON ICS^{TM} mud, even if it contains dissolved air equivalent to 15 vol % at ambient pressure. Contact angle measurements of APHRON ICS^{TM} mud on glass pre-wetted with a couple of crude oils showed that the mud will spread; the reverse situation, namely crude oil on APHRON ICS^{TM} mud produces a similar result. These tests demonstrate that the APHRON ICS^{TM} mud and crude oils are fairly compatible, i.e. the drilling fluid is not strongly hydrophilic, which is surprising for a water-based fluid. Thus, it may be expected that the mud and crude oil will intermingle and flow together easily, resulting in little potential formation damage.

In the area of Flow Properties, viscosity profiles of APHRON ICS^{TM} muds containing various amounts of air indicate that, above 10 to 15 vol % air, the high-shear-rate viscosity increases with increasing air concentration. The high-shear-rate range begins at a shear rate of about 1 rpm (1.6 sec^{-1}). Below that shear rate, all of the curves converge, so that there is little or no effect of air concentration on the low-shear-rate viscosity. The viscosity profiles at 150 ^{o}F are very similar to those at room temperature; above ~ 200 sec^{-1}, the viscosity is a little lower at 150 ^{o}F. The role of ACTIGUARD was also explored: 1 lb/bbl ACTIGUARD has no effect on bulk viscosity, though it reduces the ability of the mud to entrain air by as much as 25%. A fluid invasion model has been developed by Dr. Peter Popov of Texas A&M University, which shows that under downhole conditions the rheology of the APHRON ICS^{TM} fluid can control its depth of invasion to a couple of meters. Aphrons, particulate matter and surfactants may reduce this further, but additional work will need to be carried out to quantify those effects.

Finally, in the area of Formation Invasion and Damage Potential, linear, static Leak-Off tests at 200 ^{o}F, Fore-Pressure = 2000 psig and Back-Pressure = 1000 psig showed that Solids-Free

APHRON ICS™ fluid can seal Aloxite cores ranging in permeability from 2 to 10 Darcy; the Leak-Off is commensurate with the permeability of the core. The Solids-Free standard reservoir drilling fluid FLOPRO NT™ drilling fluid, on the other hand, is not able to seal a 2-Darcy core, even with the fluid's LSRV raised to a value comparable to that of the APHRON ICS™ fluid. With addition of 30 ppb $CaCO_3$, both fluids, when prepared in 10% NaCl, provided similar ultra-low Leak-Off; in fresh water, the Leak-Off of the APHRON ICS™ fluid was a little higher. [While the temperature and pressure specifications for these Leak-Off tests are reasonable and practical, the flow geometry (linear), fluid loading (static) and shortness of the cores (2 in) may not adequately simulate invasion of fluids like APHRON ICS™ that are thought to seal internally.]

Capillary Flow tests, along with Core Leak-Off and Modified Capillary Suction tests, indicate that the solids and surfactants in APHRON ICS drilling fluids play major roles in reducing fluid invasion in both low- and high-permeability media. While both the solids and surfactants can act as plugging agents (the surfactants perhaps through formation of macroscopic micelles), the solids can also increase bulk viscosity, while the surfactants also affect the kinetics of the flow process.

Several opportunities presented themselves to share the latest aphron drilling fluid technology with potential clients and collaborate on the Project. These included the following:

- Training seminar Jan. 12 by Jeff Buckhout of AWC on plumbing, tubing and fittings.
- Acceptance of Paper Proposal for V INGEPET in Lima, Peru, Nov. 8-11, 2005: "New Insights into Aphron Drilling Fluids."
- Meeting Jan. 27 with Cory Sikora & Mike George of Celanese on testing of potential replacements for APHRONIZER B.
- Meeting Jan. 28 with Arnis Judzis & Sid Green of Terratek on work plan for drilling simulation tests.
- Drilling Fluids Training of personnel at NETL in Morgantown, W. Va., Feb. 14 & 15.
- Annual Project Review of DOE Project at NETL in Morgantown, W. Va., Feb. 16.
- Presentation of work entitled, "Static Leak-Off Tests of APHRON ICS™ Drilling Fluids," to Eric van Oort at Shell Exploration & Production Co., New Orleans, LA, Feb. 16.
- Meeting with Cory Sikora of Celanese on testing of potential replacements for APHRONIZER B (EMI-780), Feb. 22.
- Presentation of recent findings of DOE project to M-I SWACO Tech Service, March 14.
- Tour of MASI Technologies lab and review of DOE Project for Hank Bakker, Devon Canada Corporation, March 31.
- Submission of testimony to Energy & Water Subcommittees of the House and Senate Committees on Appropriations regarding the necessity and value of the Aphron Drilling Fluids Project.
- Submission of article for May/June issue of **GasTIPS**: **"**Enhanced Wellbore Stabilization and Reservoir Productivity with Aphron Drilling Fluid Technology**."**
- Submission of article for May/June issue of **Drilling Contractor**: "US DOE-Backed R&D Validates Effectiveness of Aphron Drilling Fluids in Depleted Zones."
- Acceptance of paper and poster proposal SPE 96145 for the 2005 SPE Annual Technical Conference and Exhibition, Dallas, Texas, Oct 9-12, 2005: "How Aphron Drilling Fluids Work."

EXPERIMENTAL APPROACH

The various approaches and tools used for the three task areas of Phase II are detailed below:

4.0 Aphron Drilling Fluid Optimization

4.1. Microstructure
- 4.1.1. Chemical Composition and Morphology
- 4.1.2. Oil-Wetting/Water-Wetting Nature

4.2. Performance
- 4.2.1. Compression resistance
- 4.2.2. Elasticity
- 4.2.3. Leak-Off / Return Permeability
- 4.2.4. Capillary Suction Kinetics

The composition of the three generations of APHRON ICS™ drilling fluids are shown in Table 1.

Table 1. Composition of APHRON ICS™ Drilling Fluids

		Quantity per Lab Equivalent Barrel		
Component	**Unit**	**Standard**	**Enhanced**	**SuperEnhanced**
Water	mL	338	337	337
Soda Ash	g	3	3	3
X-CIDE	mL	0.1	0.1	0.1
GO-DEVIL II	g	5	5	5
ACTIVATOR I	g	5	5	5
ACTIVATOR II	g	2	2	2
BLUE STREAK	mL	0.91	0.91	0.91
APHRONIZER A	mL		0.5	0.5
APHRONIZER B	g		0.5	0.5
PLASTICIZER	mL			0.3

The most current of these formulations, dubbed SuperEnhanced APHRON ICS™, contains three aphron-stabilizing components: a surfactant, APHRONIZER A; a polymer, APHRONIZER B; and a fatty acid blend, PLASTICIZER (recently trade-named PLASTISIZER). However, neither the composition of this system nor the method of incorporating air into it have been optimized. In this task area, the composition of the SuperEnhanced APHRON ICS™ system and the method of generating aphrons are being varied to optimize (a) the stability of aphrons at elevated pressures and temperatures, (b) their ability to reduce leak-off, and (c) their ability to be removed

from producing reservoirs. Both the microstructure of the aphron and its behavior in drilling environments are being examined as functions of fluid composition and method of generating the aphron.

The microstructural work entails deciphering the chemical composition and morphology of the layers that constitute the presumed aphron structure. This also entails examination of the physical chemistry involved during drilling fluid invasion and back-flow of produced fluid from permeable formations. Interactions among all of the phases involved (drilling fluid, produced fluid, mineral surfaces and aphrons) are studied using methods developed in Phase I and under development in Phase II to quantify hydrophobicity of bubbles.

Complementing the microstructural investigation are performance tests that include some microscopic techniques developed in Phase I, such as Bubble Compression Resistance (kinetics of bubble shrinkage at elevated pressure) and Elasticity (transient response of bubble size to rapid pressure changes). Macroscopic tests include Leak-Off, Return Permeability and Capillary Suction Time.

Aphron Microstructure and Morphology

Initial efforts to optimize the drilling fluid formulation consist of preparing 16 "modified" SuperEnhanced APHRON ICS™ fluid formulations using high and low levels each of GO-DEVIL II, APHRONIZER A, APHRONIZER B and PLASTISIZER. Aphron survivability is determined by monitoring the full bubble size distribution (BSD) at 500 psig (3.5 MPa), as well as by measuring the rate of shrinkage of individual aphrons at that pressure. The high-pressure Variable Reservoir Depth viewing cell shown in Figure 1 is being used for all of the observations.

Accurate BSD's are being generated with the NI Vision Assistant software, and a mathematical model is being developed to describe and correlate the relationship between composition and bubble stability.

Figure 2. Polycarbonate VRD Viewing Cell

Front View of Cell

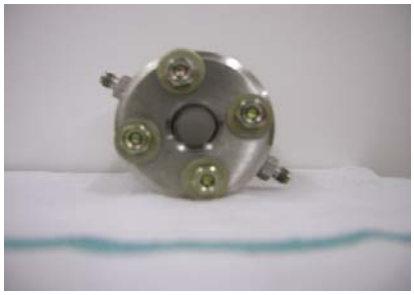

Side View of Cell

Disassembled Cell

Method of Generating Aphrons

Various laboratory mixers and flow/pressure drop through an orifice were examined to determine if there is any effect of the method of generating aphrons on bubble stability. The Prince Castle Mixer (see Figure 3) is commonly found in drilling fluid laboratories and in the food industry; the APV Gaulin Homogenizer (Figure 4) is not generally used to mix drilling fluids, but is common in the food and dairy industries. The latter pumps the fluid with a reciprocating piston that applies a pressure drop of 500 to 4500 psig (3.5 to 30.7 MPa) to the sample.

The effect of submitting aphron drilling fluids to a pressure drop was also investigated. The experiment was set up in the HTHP Circulating System, as shown in Figure 5. The Canty Viewing Cell was modified by inserting a tube with a 1-mm diameter opening into the bottom port of the

cell. A pressure drop is applied across the orifice while maintaining the pressure in the viewing chamber at a pressure of 500 to 2000 psig (3.5 to 13.7 MPa).

Figure 3. Prince Castle Mixer

Figure 4. APV Gaulin Homogenizer

Figure 5. Set-Up for Pressure Drop Tests in Canty Viewing Cell

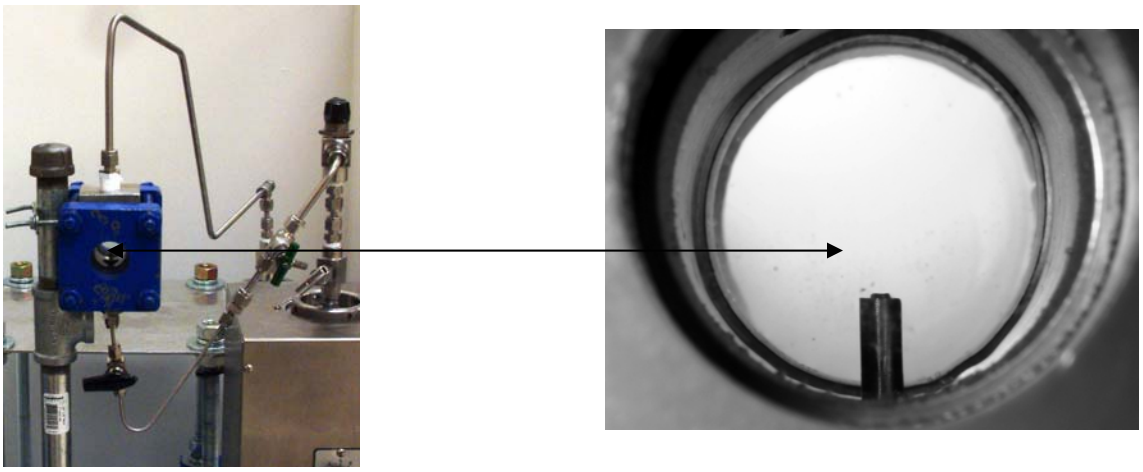

Surface Chemistry of Aphron Drilling Fluids

During drilling fluid invasion and subsequent production of oil or gas, base drilling fluid, aphrons, pore walls and produced fluid interact in various ways to determine the extent of invasion and formation damage. These include the following:

(1) Bubble-Bubble

(2) Bubble-Mineral Surface (Pore Wall)

(3) Drilling Fluid-Produced Fluid (Produced Fluid includes connate water, oil or gas)

(4) Bubble-Drilling Fluid (Drilling Fluid is defined here as the aqueous phase surrounding the aphrons)

(5) Drilling Fluid-Mineral Surface

(6) Produced Fluid-Mineral Surface

All of the interactions above, save those involving Produced Fluid, will be studied with 2-D Visualization. For this purpose, a modified Hele-Shaw cell[7] was constructed to observe how bubbles move through unconsolidated beds of sands. The walls, which have a fixed gap of 10 mm, are made of Lexan (polycarbonate). Initially the cell was packed with 5-mm glass beads and filled with water, as shown in Figure 6.

Figure 6. Modified Hele-Shaw Cell Packed with 5mm-glass beads

This new cell is smaller, sturdier, easier to clean and more transparent than the Hele-Shaw cell and "ant farm" devices used previously.

Other techniques used in these studies include Contact Angle Goniometry (interactions (3) – (6)), Emulsion Compatibility (interaction (3)) and Surface Tensiometry (interaction (4)). For Contact Angle Goniometry, the Sessile Drop technique described in API RP 42 was adopted initially. A preliminary set-up of the apparatus containing a sample of SuperEnhanced APHRON ICS™ fluid is shown in Figure 7.

Figure 7. Sessile Drop Contact Angle Apparatus

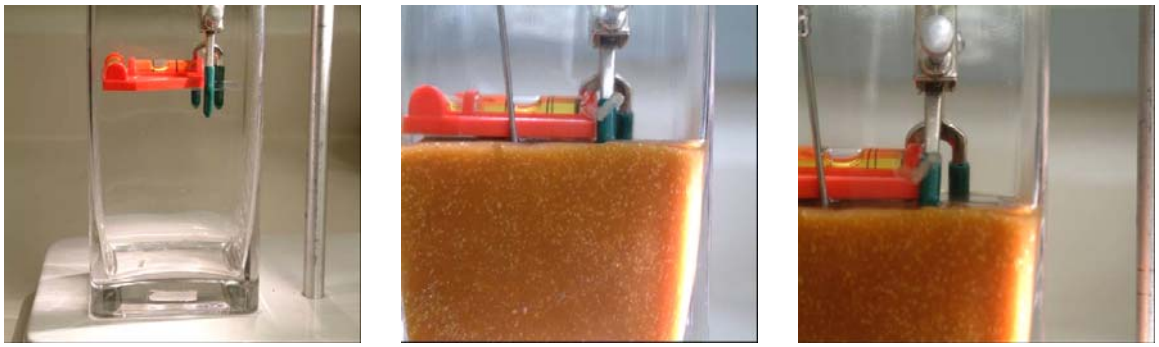

The clamp holds the microscope slide in place. The orange Level is used only to ensure that the slide is horizontal. The tube coming down into the mud is actually a syringe needle, which is bent upward and is used to dispense a drop of a low-density fluid, e.g. oil, to the underside of the microscope slide. As it stands, the Sessile Drop Apparatus does not permit looking through opaque fluids. Consequently, a transparent version of the APHRON ICS™ fluid system was used, and this was centrifuged to remove aphrons. In addition, a darker oil supplanted the nearly colorless oil used before, thus providing sufficient contrast between the oil droplet and the drilling fluid. A couple of pictures of the Sessile Drop Apparatus with these modifications are shown in Figure 8.

Due to the high viscosity of the oil and of the mud, it was very difficult for the oil droplet to assume its equilibrium circular shape and enable accurate measurement of the contact angle. Here the oil droplets on the underside of the microscope slide appear to be “comma”-shaped.

Figure 8: Sessile Drop Apparatus: Dark Oil and Transparent APHRON ICS™ Mud

Two additional modifications were made. The first was to decrease the viscosities of both the mud and oil. For this purpose, the mud was diluted 50:50 by volume with water, and a less viscous crude oil was substituted for the dark crude. The pictures in Figure 9 show what happened.

Figure 9. Sessile Drop Apparatus with Light Oil and Diluted APHRON ICS™ mud

Although the oil droplet produced a fine, nearly circular pattern on the slide, absence of a suitable optical train made it very difficult to quantify the contact angle. Consequently, the Sessile Drop method was abandoned in favor of a Microscope Slide Smear. The slide was pre-wetted with the whole SuperEnhanced APHRON ICS™ mud, and a drop of crude oil was placed on its

surface. The converse was also attempted, i.e. pre-wetting the slide with the oil and placing a drop of the mud on its surface.

At the conclusion of these studies, we expect to have a fairly comprehensive picture of the physical chemistry involved in drilling fluid invasion and reservoir fluid production. Some of these data will also be used for the Bubbly Flow modeling that will be conducted at Texas A&M University.

5.0 Flow Properties

5.1. Fluid Flow Pattern
  5.1.1. Core Geometry
  5.1.2. Dynamic vs Static Fluid Flow
5.2. Fluid Rheology
5.3. Multi-Phase Flow Effects

The low invasion rate of aphron drilling fluids into simulated permeable and fractured rock that was previously documented appears to be related to the very high LSRV of the drilling fluid and to acceleration of the pressure-stable aphrons ahead of the liquid front.[4] However, thus far these tests have been carried out only with a fixed fluid reservoir using linear flow. It is imperative that we re-examine the flow properties of the fluids and repeat the fluid invasion tests with a continuous source of aphrons at constant concentration, elevated pressure and in radial flow (as occurs in a wellbore).

Fluid Flow Pattern

As a continuation of the study to understand the Leak-Off behavior of the fluid, this project takes the study one step further from the linear to radial flow.

The final goal is the measurement of the radial Leak-Off. As a first approach, the construction of a semi-circular transparent cell is required, to get an idea of the radial flow at ambient pressure and temperature.

The cell is going to be packed with sand. Dynamic drilling like flow is simulated, and the front of the fluid observed and recorded. The bubbly flow phenomenon is expected to occur. This means, the air bubbles are expected to migrate to the front of flow.

A schematic of the Radial Flow Apparatus is shown in Figure 10. The device incorporates dynamic flow at the fluid inlet (wellbore side) and a long path length for the fluid (sand pack is over 2 ft long), along with radial flow. An Oberdorfer variable speed ¾ hp progressive cavity pump provides the required movement of all the fluids. The walls of the Apparatus are made of Lexan (polycarbonate plastic) glued together and supported with clamps that minimize swelling and bending of the plastic when subjected to pressure. The entire apparatus sits atop a light box of similar dimensions that contains several 7-W and 13-W 4100 ^{o}K fluorescent lights. The system contains water initially, which is replaced with mud at the beginning of a test. A Sony DCR-HC90 Digital MiniDV camcorder will be attached to a rail that permits rack and pinion X-Y movement, thus enabling the camera to traverse the length and width of the apparatus without the need to re-focus.

Figure 10. Schematic of Radial Flow Apparatus

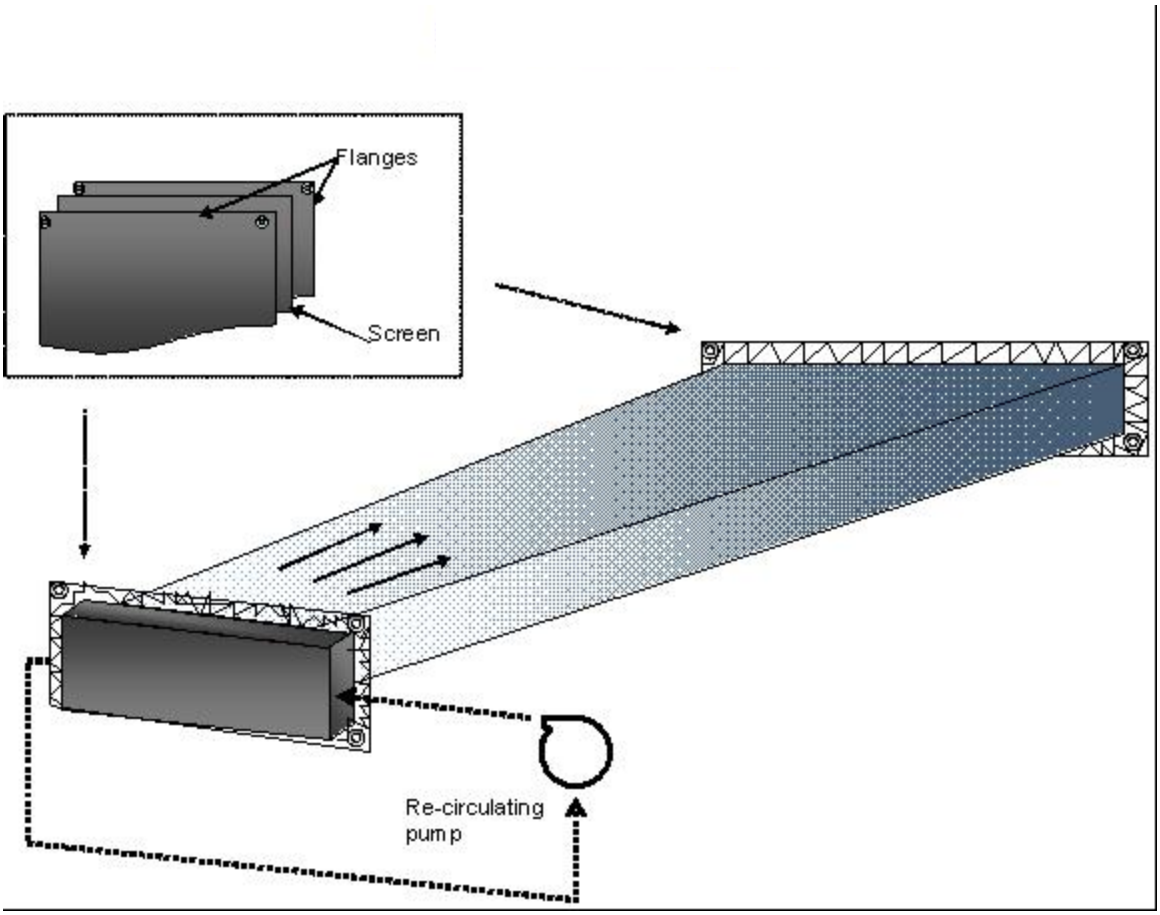

Mud is circulated continuously to the system at the face of the sand pack (simulating the drilling process). The flowing mud invades the sand pack and advances radially to the end of the cell, where it is collected and weighed regularly.

Complementing the study on Leak-Off behavior of aphron drilling fluids, which imposes linear flow through permeable cores, this project takes that work another important step: radial flow. Construction of the Radial Flow Apparatus was completed during this last Quarter, but in the first attempts to push mud through a pack of glass beads, several leaks were found. Some modifications have been made to the system to eliminate leaks, and a water reservoir was added to permit sufficient flushing of the system prior to running a displacement test. The latest version of the system is shown in Figures 11 and 12.

Figure 11. Radial Flow Apparatus

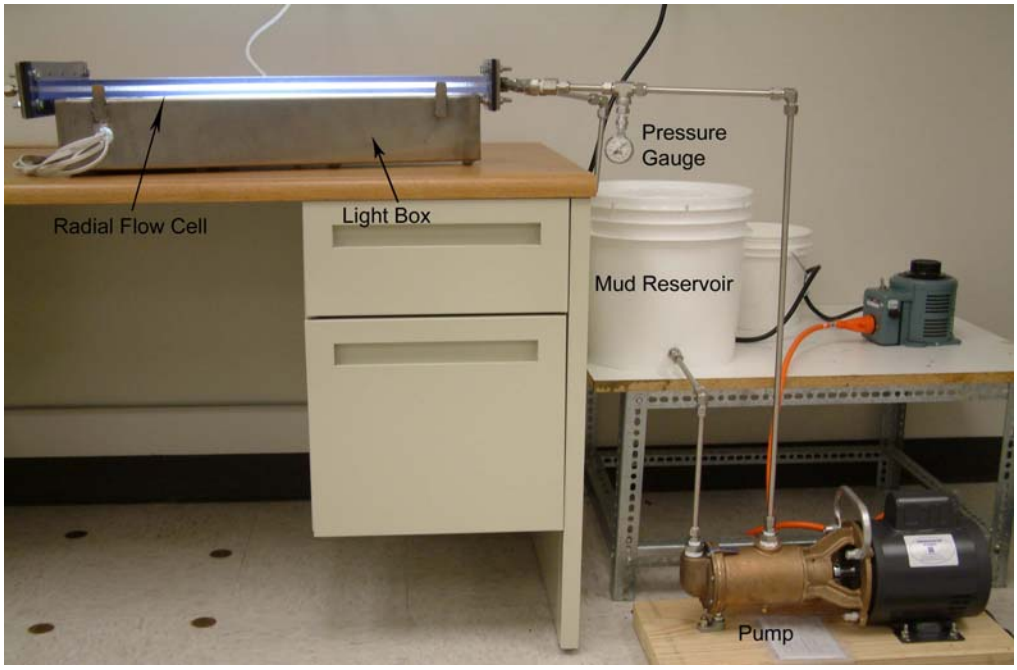

The next steps include adding some additional plumbing to permit swapping out flow of water for flow of mud. The first tests will be conducted with SE APHRON ICS™ mud displacing water through a bed of glass beads, similar to the Hele-Shaw cell tests described above.

Figure 12. Radial Flow Cell

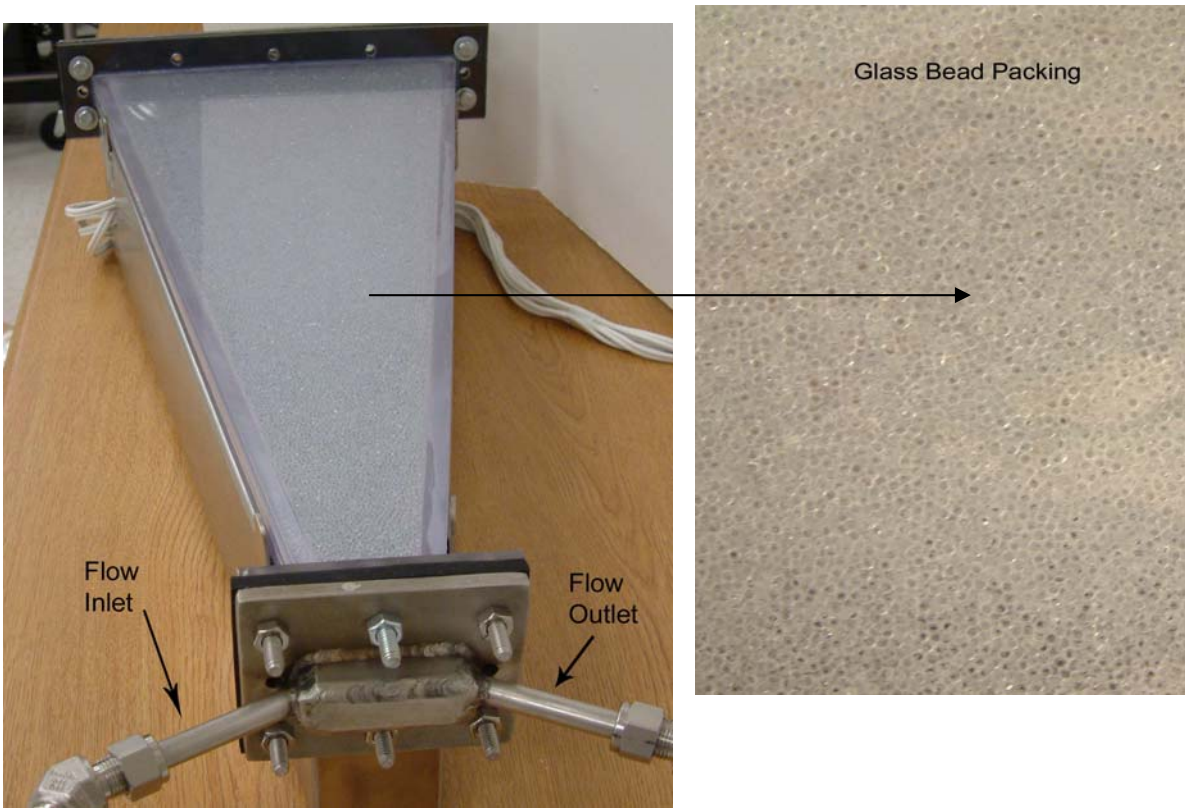

Fluid Rheology

Shear viscosity of the aphron drilling fluids is being measured with a Grace M3500 viscosimeter at ambient temperature and pressure over the shear rate range 0.01 to 1000 sec^{-1}. This covers the standard Fann 35 viscosimeter shear rate range of 5 to 1000 sec^{-1}, as well as the Brookfield viscosimeter LSRV measurements at 0.06 sec^{-1}. The effects of air concentration (up to about 60 vol %) and bubble size distribution (BSD) on the viscosity of the base fluid are being examined first.

In addition, unconventional rheology of aphron drilling fluids, such as extensional viscosity, is beginning to be examined at CP Kelco in San Diego, CA, to determine what role – if any – such properties may play in the flow of aphron drilling fluids through porous media.

Multi-Phase Flow Effects

Dr. Peter Popov of Texas A&M University has begun development of a Bubbly Flow model for aphron drilling fluids; using the shear viscosity profile of the base APHRON ICS™ fluid over the shear rate range 0.01 to 1000 sec^{-1}, he has formulated fluid invasion profiles for low-viscosity (high shear rate) and high-viscosity (low shear rate) boundary cases, assuming Darcy flow. Now he is adding bubbles to the system under these conditions (see Fluid Rheology section above), and the effects of air concentration and BSD on viscosity will be incorporated into the model.

6.0 Formation Invasion and Damage Potential

6.1. Laboratory Tests of Core Leak-Off and Return Permeability
6.2. Field Simulation Tests

Static Linear Leak-Off Tests

Shell Exploration and Production Company Oil has requested some conventional competitive Leak-Off tests of the APHRON ICS™ and FLOPRO NT™ systems at elevated temperature and pressure, using a range of Back-Pressures, and with synthetic cores covering a broad range of permeability.

Static Leak-Off tests were conducted using linear flow through Aloxite cores 1-1/2 in (3.8 cm) diameter x 2 in (5.1 cm) length at 200 ^{o}F (93 ^{o}C) and 2,000 psig (13.7 MPa) Fore-Pressure. Confining pressure was maintained at 2,500 psig (17.3 MPa). A schematic of the Triaxial Core Leak-Off Tester is shown in Figure 13. Back-Pressure was maintained by a high-pressure diaphragm-type Back-Pressure regulator and an additional ISCO syringe pump.

The Leak-Off tests were run for a period of 30 min, and the weight of filtrate collected was monitored in real time. Several tests were run in duplicate, and reproducibility of the Leak-Off values was found to be 1 to 6 mL for Leak-Offs of 2 to 40 mL, respectively.

Figure 13. Schematic of Triaxial Core Leak-Off Tester

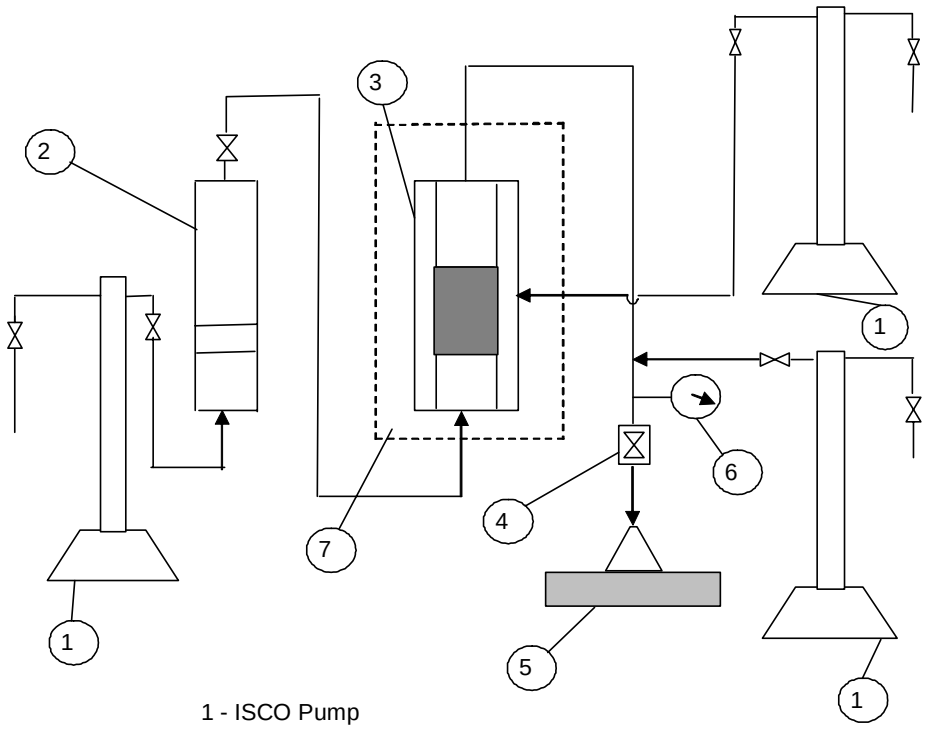

1 - ISCO Pump
2 - Accumulator with Piston
3 - Temco Coreholder with Core
4 - Back-Pressure Regulator
5 - Balance
6 - Pressure Gauge
7 - Oven

While the temperature and pressure specifications of the Leak-Off tests are reasonable and practical, the fluid loading method (static), shortness of the cores (2 in) and flow geometry (linear) are suitable only for fluids that build an external filter cake. APHRON ICS™ drilling fluids, which are expected to form an internal seal in loss zones,[1] require a design that simulates erosion of the filter cake and dynamic loading of aphrons into the formation, longer cores and radial geometry (as in a wellbore) to better simulate expansion of the internal phase. The Radial Flow Apparatus that was recently constructed (see Section **5.0 Flow Properties** – Fluid Flow Pattern) will incorporate these design specifications.

Flow of Drilling Fluid in Capillaries

Microbore stainless steel tubing 5 ft long (1.52 m) and 1/8-in (3.18 mm) OD was used to simulate long – though not tortuous -- pores in a reservoir. Two tubing ID's were used: 0.01 in (0.25 mm) and 0.005 in (0.127 mm). The APHRON ICS™ fluid was constructed from its individual components, rather than the branded products, and the effect of each component was determined by omitting it from the mix. The system was pumped through the tubing with an ISCO D500 syringe pump using a pressure ramp, and the flow rate was recorded as a function of pressure. The experimental set up is shown in Figure 14.

Figure 14. Capillary Flow Test Apparatus

RESULTS AND DISCUSSION

4.0 Aphron Drilling Fluid Optimization

Chemical Composition and Morphology

Optimization of the APHRON ICS™ drilling fluid formulation was continued this Quarter with additional performance tests. The test matrix currently being investigated includes 16 formulations with varying concentrations of GO-DEVIL II and the three aphron stabilizers APHRONIZER A, APHRONIZER B and PLASTISIZER (sic), as shown in Table 2. Aphron survivability is being determined by monitoring the full bubble size distribution (BSD) at 500 psig, as well as by measurement of the rate of shrinkage of individual aphrons at that pressure.

Table 2. Test Matrix for Optimization of APHRON ICS™ Drilling Fluid Composition

Formulation	Soda Ash (ppb)	X-Cide (ppb)	Activator II (ppb)	Go-Devil (ppb)	Activator I (ppb)	Blue Streak (ppb)	Aphronizer A (ppb)	Aphronizer B (ppb)	Plasticizer (ppb)
1	3	0.1	2	3.5	5	1	0.25	0.25	0.2
2	3	0.1	2	5	5	1	0.25	0.25	0.2
3	3	0.1	2	3.5	5	1	0.25	0.25	0.4
4	3	0.1	2	5	5	1	0.25	0.25	0.4
5	3	0.1	2	3.5	5	1	0.25	0.6	0.2
6	3	0.1	2	5	5	1	0.25	0.6	0.2
7	3	0.1	2	3.5	5	1	0.25	0.6	0.4
8	3	0.1	2	5	5	1	0.25	0.6	0.4
9	3	0.1	2	3.5	5	1	0.75	0.25	0.2
10	3	0.1	2	5	5	1	0.75	0.25	0.2
11	3	0.1	2	3.5	5	1	0.75	0.25	0.4
12	3	0.1	2	5	5	1	0.75	0.25	0.4
13	3	0.1	2	3.5	5	1	0.75	0.6	0.2
14	3	0.1	2	5	5	1	0.75	0.6	0.2
15	3	0.1	2	3.5	5	1	0.75	0.6	0.4
16	3	0.1	2	5	5	1	0.75	0.6	0.4

A typical example is Formulation #8, with 0.25 ppb APHRONIZER A, 0.6 ppb APHRONIZER B and 0.4 ppb PLASTISIZER (compared to the standard formulation which contains 0.5, 0.5 and 0.3 ppb, respectively, of these products). Figure 15 shows the effect of pressurizing this sample to 500 psig. Through the application of the image analysis software NI Vision Assistant, BSD's can be generated in the form of Differential Volume, Cumulative Volume or # Bubbles vs Size. The Total Volume of Air in the sample can be obtained by integrating the Differential Volume curve. For example, in Formulation #8 at 500 psig, the Total Volume of Air calculated via image analysis is 0.45 vol %. This compares quite favorably with the volume of air predicted from

application of Boyle's Law to the measured initial volume of air: $V_{final} = P_{initial}V_{initia}l/V_{final}$, i.e. 15 vol % at ambient pressure (14.7 psia) is reduced to 0.42 vol % at 500 psig (514.7 psia).

Figure 15. Image of APHRON ICS™ Formulation #8 Compressed to 500 psig

P = Ambient, T = Ambient **P = 500 psig, T = Ambient**

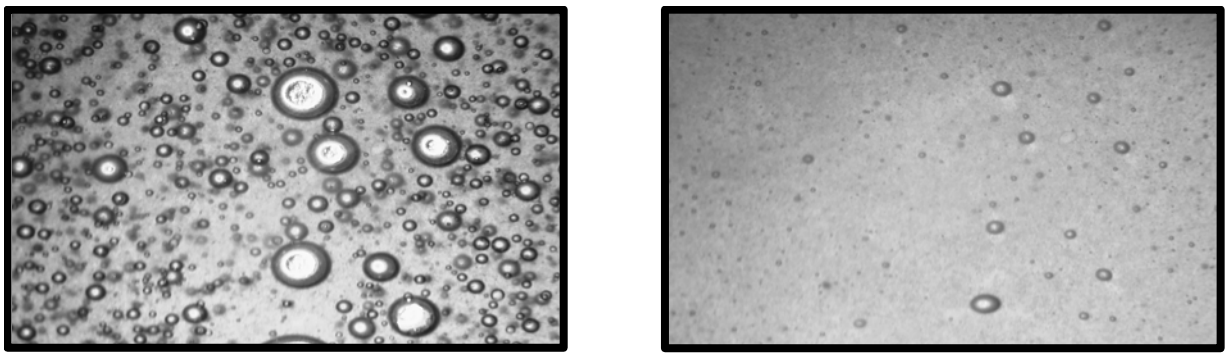

Shown in Figures 16 and 17 are examples of BSD's that were determined for Formulation #8 and Formulation #15 at 500 psig immediately after pressurization and 10 minutes later. One can clearly see how many aphrons survived and how they shrunk over the 10-min period.

Figure 16. Survivability of Aphrons in Formulation #8

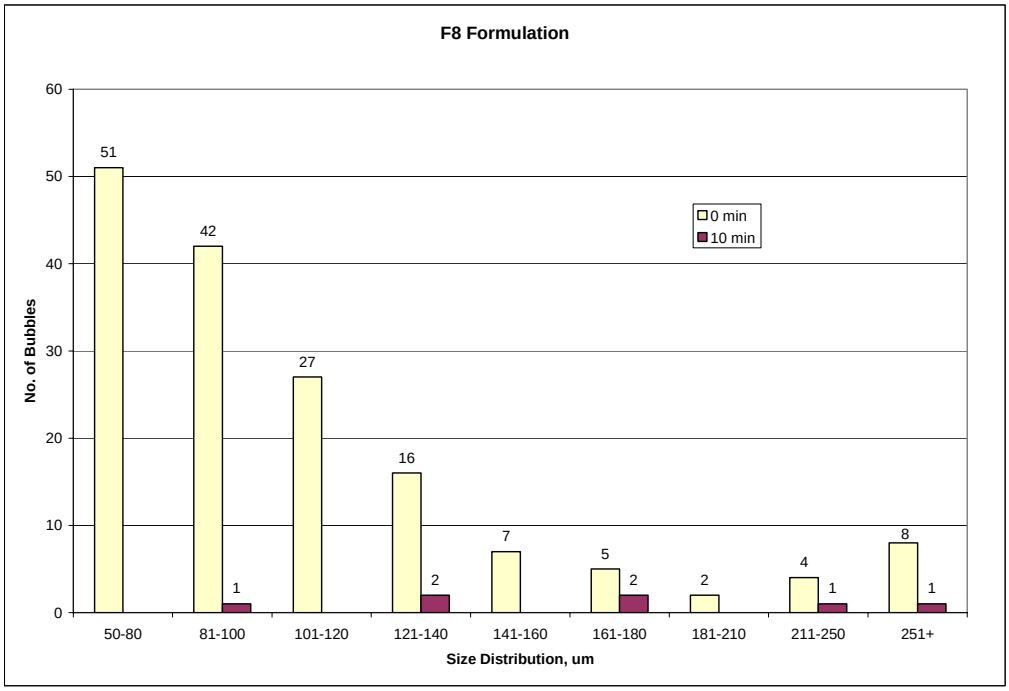

Figure 17. Survivability of Aphrons in Formulation # 15

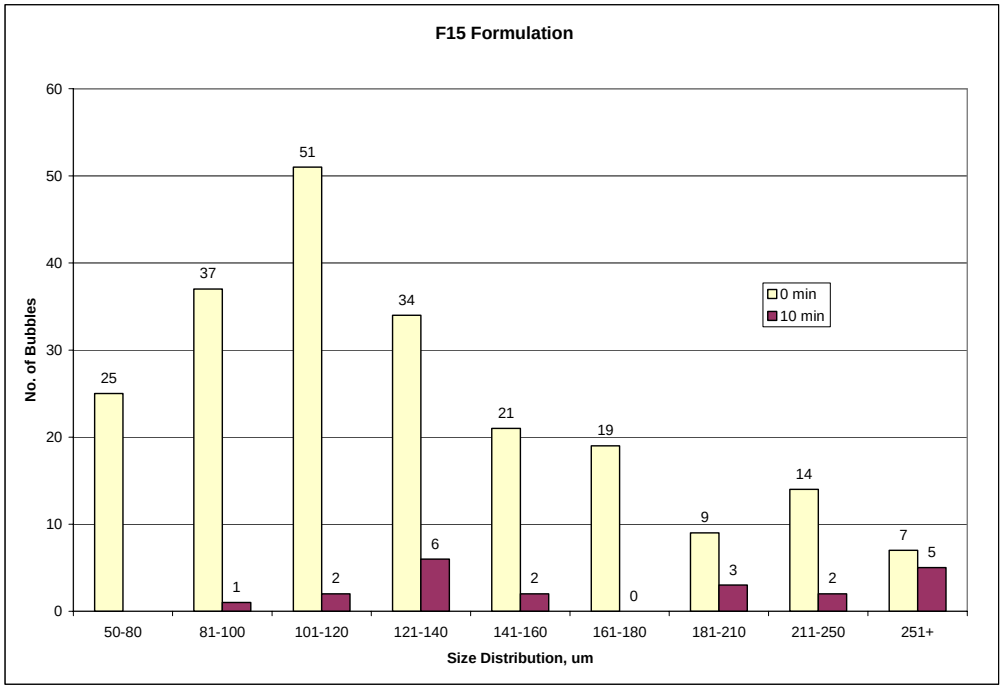

It will be noted that no aphrons were observed that were smaller than 50 μm diameter, consistent with our previous observations and those of Sebba.[5] It is clear from this initial optimization study that, as stable as the aphrons may be in the current APHRON ICS™ drilling fluid, even greater stability is highly desirable. All 16 formulations are being compared to determine if there is a correlation between composition and change in overall BSD or some parameter that can be derived from the BSD, such as the change in D_{50}. Initial analysis suggests that reducing the concentration of GO-DEVIL II and increasing the concentration of PLASTISIZER increases bubble stability. Unfortunately, the method of generating the aphrons in the first place did not produce a consistent initial BSD or amount of entrained air. A more promising alternative is the kinetics of shrinkage of a single bubble of some pre-defined size; this will be looked at during the next Quarter, along with other performance measures before making any recommendations to change the existing APHRON ICS™ formulation. At the conclusion of this study, alternative materials will be examined as additives or as substitutes for existing components.

Method of Generating Aphrons

During the last Quarter, it was determined that the Silverson L4RTW and Prince Castle mixers produced SuperEnhanced APHRON ICS™ drilling fluids with similar physical properties, BSD and aphron stability, and that these were superior to the drilling fluids produced with a General Electric kitchen blender. A comparison was made this Quarter of the Prince Castle mixer and the APV Gaulin Homogenizer, i.e. shear with a single spindle mixer versus shear / cavitation / extension with a pressure-drop pump. The following operating parameters were used: (a) the Prince Castle mixer at 7,000 rpm for 6 min, (b) the Gaulin Homogenizer with one pass (fluid pumped through once) at 4,000 psig and (c) the Gaulin Homogenizer with recirculation for 2 minutes at 4000 psig. Some significantly different mud properties were observed from these three treatments, particularly with regard to Brookfield viscosity and BSD. After only one pass, the Gaulin Homogenizer reduced the LSRV of the fluid significantly and produced a smaller BSD than the Prince Castle mixer; with multiple passes, the LSRV dropped by an order of magnitude.

Nevertheless, it was considered instructive to examine in closer detail the effects of subjecting the APHRON ICS™ mud to a pressure drop, though one designed to simulate more closely downhole conditions. For this purpose, a simple 1-mm orifice was installed in the Canty Viewing Cell of the HTHP Circulating System; the inlet pressure was maintained at 2000 psig in all cases, while the Viewing Cell was maintained at 0 or 1500 psig, i.e. ΔP = 500 or 2000 psi instead of the 4000 psi of the Gaulin Homogenizer. The specifications of the tests were as follows:

- Test #1: Injection of aerated mud at 2000 psig through a 1000-µm orifice into the Viewing Cell filled with de-aerated mud at ambient pressure. Results are shown in Figure 18.
- Test #2: Injection of de-aerated mud at 2000 psig through a 500-µm orifice into the Viewing Cell filled with de-aerated mud at 1500 psig. See Figure 19.
- Test #3: Injection of aerated mud, held at 2000 psig for 2 min, through a 500-µm orifice into the Viewing Cell filled with de-aerated mud at 1500 psig. See Figure 20.

These photos indicate that, if the mud system already contains undissolved air (aphrons), a pressure drop can induce the aphrons to expand and perhaps even form new ones (Test #3, Figure 20). However, when the mud is de-aerated via centrifugation and injected at 2000 psig into de-aerated mud at 1500 psig (Test #2, Figure 19), aphrons are not formed.

Figure 18. Injection of Aerated Mud at 2000 psig into De-Aerated Mud at 0 psig

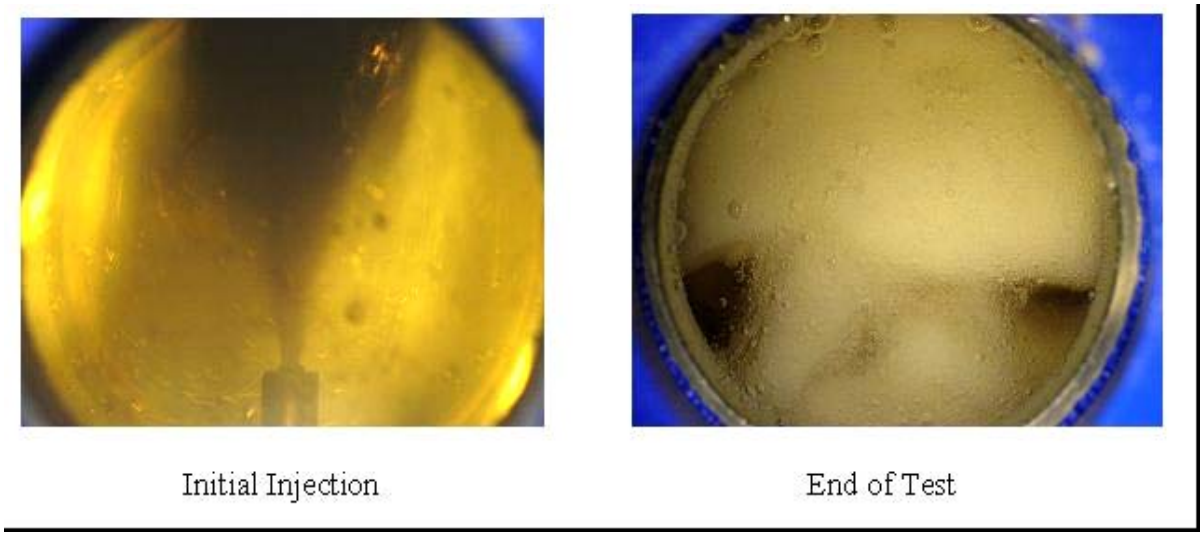

Figure 19. Injection of Deaerated Mud at 2000 psig into Deaerated Mud at 1500 psig

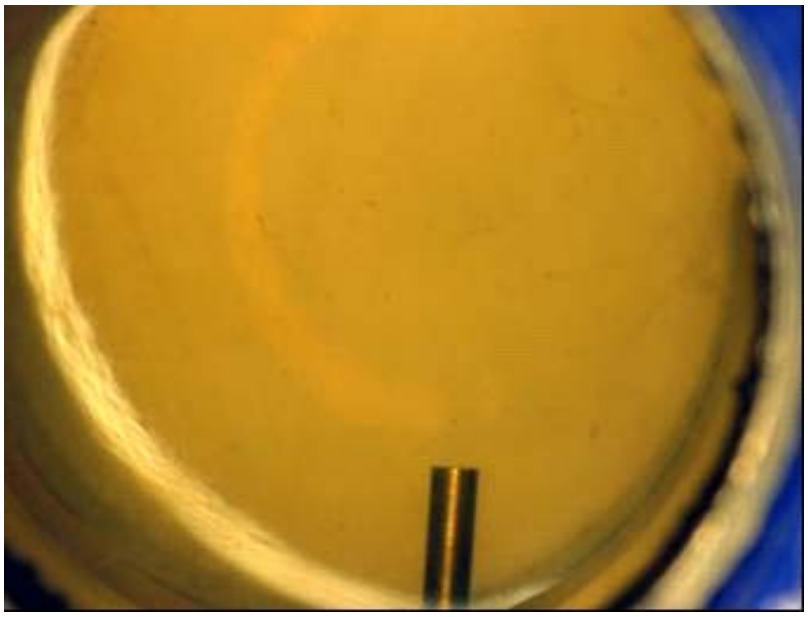

Figure 20. Injection of Aerated Mud Held at 2000 psig for 2 min into De-aerated Mud at 1500 psig

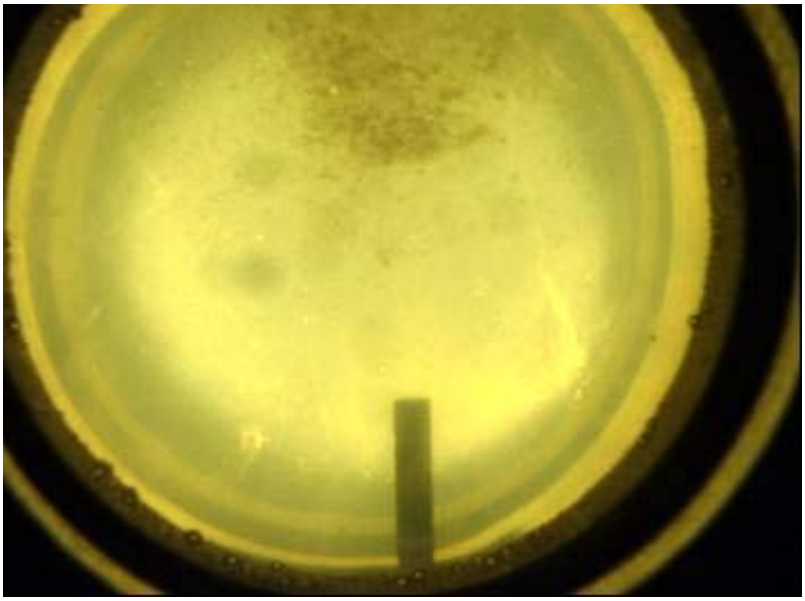

A modification of Test #3 was carried out, the difference being that the mud was held at 2000 psig for 15 min instead of 2 min. Within that time frame, most of the aphrons were expected to have degraded to such an extent that very few of them would still be around. The results are shown in Figure 21.

Very few aphrons were observed exiting the orifice, indicating that aphrons cannot be created from dissolved air if the pressure on the low side (1500 psig in this case) is sufficiently high that the system is under-saturated with air. Indeed, the system pressure must drop below the point where the concentration of air in solution exceeds the solubility limit. Thus, a pressure drop alone is not sufficient to create aphrons, though the system may contain (dissolved) air.

Figure 21. Injection of Aerated Mud Held at 2000 psig for 15 min into De-aerated Mud at 1500 psig

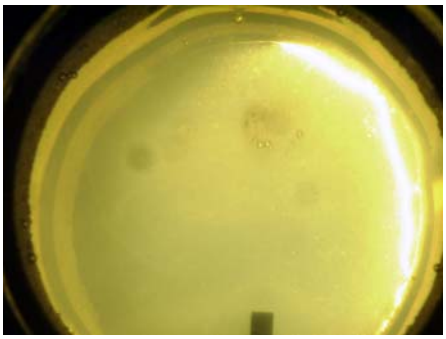

Figure 1:

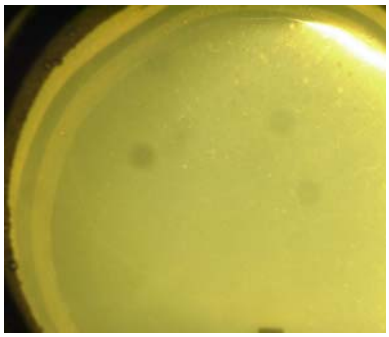

Figure 2:

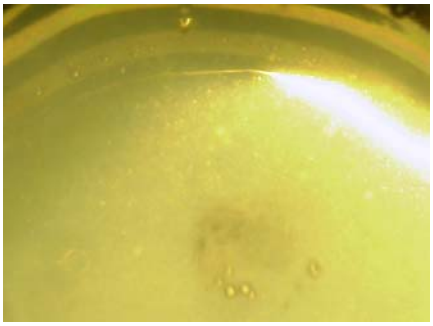

Figure 3: Figure 1 Enlarged

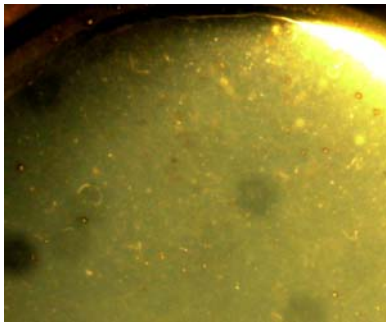

Figure 4: Figure 2 Enlarged

Physical Chemistry of Aphron Drilling Fluids

Experiments were carried out in the new Hele-Shaw cell to determine how drilling fluid and aphrons move through beds of glass beads and sand. In the first tests, the cell was packed tightly with 5-mm glass beads, the system was filled with tap water and SE APHRON ICS™ mud was pumped slowly through, displacing the water. A few pictures of the displacement – from left to right -- are shown in Figure 22.

It is apparent from the nature of the fluid front that the mud is moving in plug flow; as expected for a fluid with such high viscosity, the APHRON ICS™ mud presents a uniform flat front and there is little or no mixing with the connate water. Movies of the displacement will be made to observe the dynamics of the interaction of the mud with water and the flow pattern of the bubbles through the mud to the fluid front.

Figure 22. Displacement of Water by SE APHRON ICS™ Mud at Room Temperature and Pressure in Modified Hele-Shaw Cell Packed with 5-mm Glass Beads

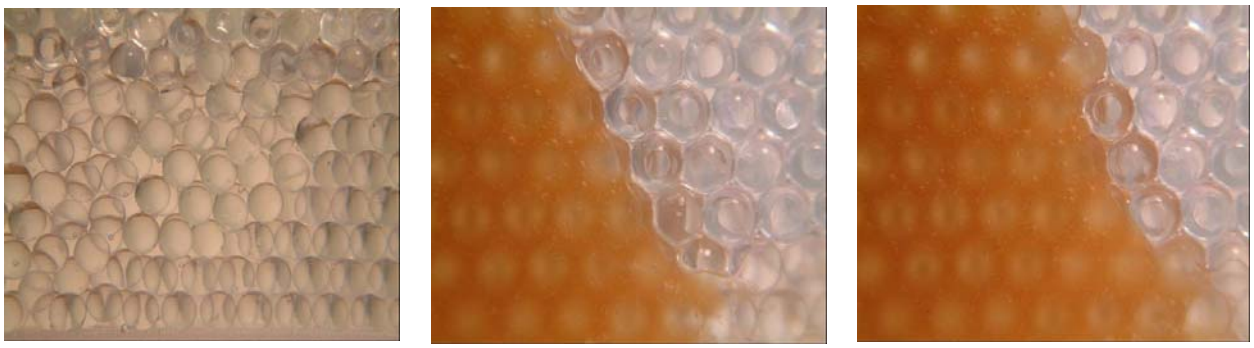

The interaction of the SE APHRON ICS™ mud with Crude Oil was investigated with some contact angle measurements on a glass microscope slide. As shown in an edge-view of the slide in Figure 23, high-viscosity Canadian Crude Oil will spread on a quartz slide pre-wetted with SE APHRON ICS™ mud. A top view (from above) of the slide is shown in Figure 24.

Figure 23. Edge View of Canadian Crude Oil Drop on Glass Slide Pre-Wetted with SE APHRON ICS™ Mud

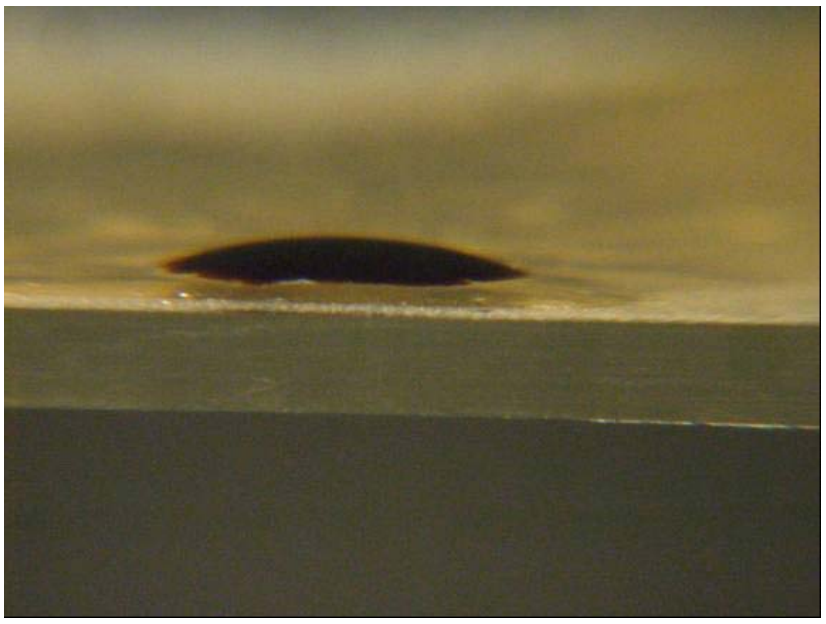

Figure 24: Top View of Canadian Crude Oil Drops on Glass Slide Pre-Wetted with SE APHRON ICS™ Mud [The picture on the right is a magnified view of the lower drop taken a few minutes later]

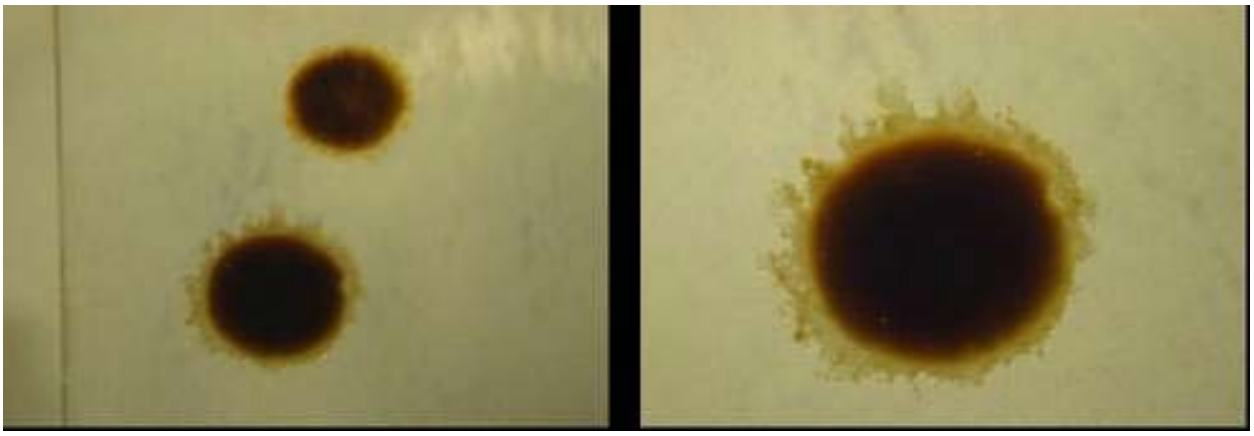

The slide in Figures 23 and 24 was immersed in whole SuperEnhanced APHRON ICS™ mud and removed, leaving a fairly uniform film of mud on the slide. Two drops of crude oil were then transferred gently from a pipette to the pre-wetted surface. Figures 23 and 24 show that the oil spreads fairly well on the mud-covered slide. The converse was also attempted, i.e. pre-wetting the slide with the oil and placing a drop of the mud on its surface. A top view of the slide is shown in Figure 25. In a side view (not shown), it is clear that the mud spreads fairly easily over the oil.

Figure 25. SE APHRON ICS™ Mud Drop on Glass Slide Pre-Wetted with Crude Oil

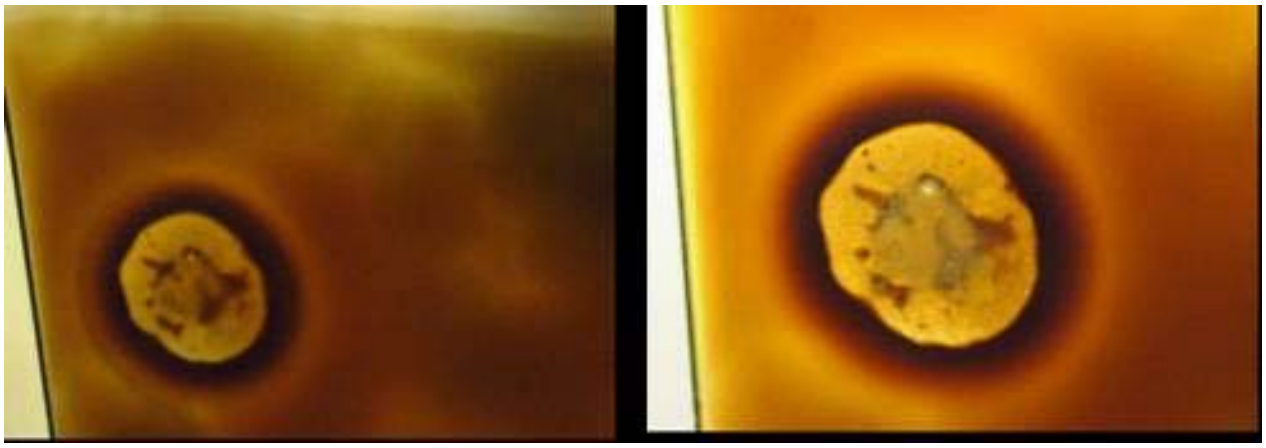

Figures 23 -25 demonstrate that the APHRON ICS™ mud and the Canadian Crude Oil are fairly compatible, i.e. the drilling fluid is not strongly hydrophilic, which is surprising for a water-based fluid. Thus, it may be expected that the mud and crude oil will intermingle and flow together easily. This will be investigated further during the following Quarter, as will the wetting of the Crude Oil and SE APHRON ICS™ mud on bare and water-wetted glass and sand.

5.0 Flow Properties

Fluid Rheology

Effect of Air Content:

To vary the amount of air in a sample while maintaining similar bubble size distributions (BSD), both the mixing method and the concentration of the primary surfactant, BLUE STREAK, had to be varied. The SuperEnhanced (SE) APHRON ICS™ formulation was used for all the tests, and all were mixed initially with the Prince Castle mixer and hot-rolled overnight at 150 ^{o}F. For samples containing up to 23% v/v air, the air was entrained with the Silverson L4RTW mixer (6 min at 9,000 rpm). The Silverson itself was not able to incorporate higher concentrations of air. For higher levels of air, a kitchen blender was used (for 1 min), followed by mixing with the Prince Castle mixer (6 min at 9,900 rpm). The concentration of BLUE STREAK was varied as follows:

Air Concentration (% v/v)	BLUE STREAK Concentration (lb/bbl)
0 to 16	1
17 to 23	2
24 to 57	3

Rheology profiles covering the range 600 to 0.01 rpm were measured at ambient temperature using a Grace M3500 viscosimeter. Calibration of the Grace M3500 viscosimeter demonstrates that, for APHRON ICS™ drilling fluids, the Grace viscosimeter provides accurate viscosities over the desired shear rate range (1000 to 0.016 sec-1), so there is no need to use two different instruments: Fann 35 or Grace M3500 for shear rates between 1.6 and 1000 sec^{-1} and a Brookfield for shear rates around 0.06 sec^{-1}).

Figure 26 shows the viscosity profiles obtained for all of the samples plotted in typical fashion of Fann Reading vs Fann Speed, and covering the normal range for drilling fluids of 3 to 600 rpm (5 to 1000 sec^{-1}).

Figure 26. Effect of Air Concentration on Viscosity of SE APHRON ICS™ Fluid

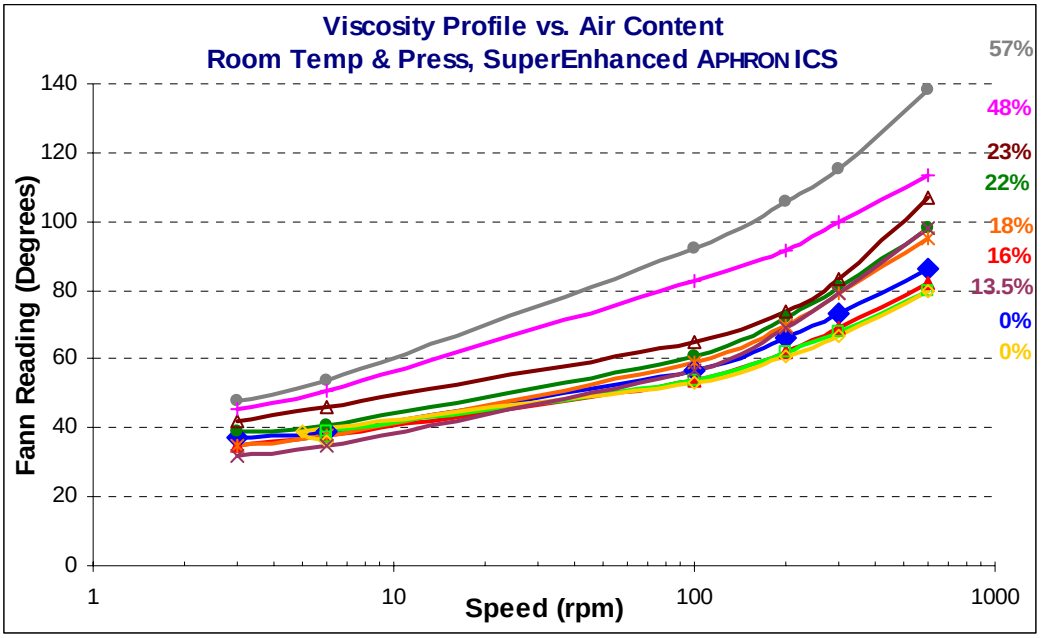

From the data in Figure 26, it appears that there is a general tendency of the high-shear-rate rheology to increase with increasing concentration of air. However, there is a threshold air concentration, on the order of 16 to 18% v/v, below which there appears to be little or no effect. This is confirmed in Figure 27, which extends the data down to a shear rate of 0.01 rpm (0.016 sec^{-1}). Several of the data sets, e.g. 13.5% v/v air, have been removed for clarity.

Here it is clear that the high-shear-rate viscosity increases with increasing air concentration, beginning with about 18% v/v air. The high-shear-rate range begins at a shear rate of about 1 rpm (1.6 sec^{-1}). Below that shear rate, all of the curves converge, so that there is little or no effect of air concentration on the low-shear-rate viscosity. The low shear rate data are expanded in Figure 28. The apparent discrepancy of the 23% is thought to be due to an error in the calibration of the viscosimeter, which shifted all of the Fann Readings upward by about 5 degrees.

Figure 27. Viscosity Profiles of SE APHRON ICS™ Fluids: [Air] = 0 – 57%

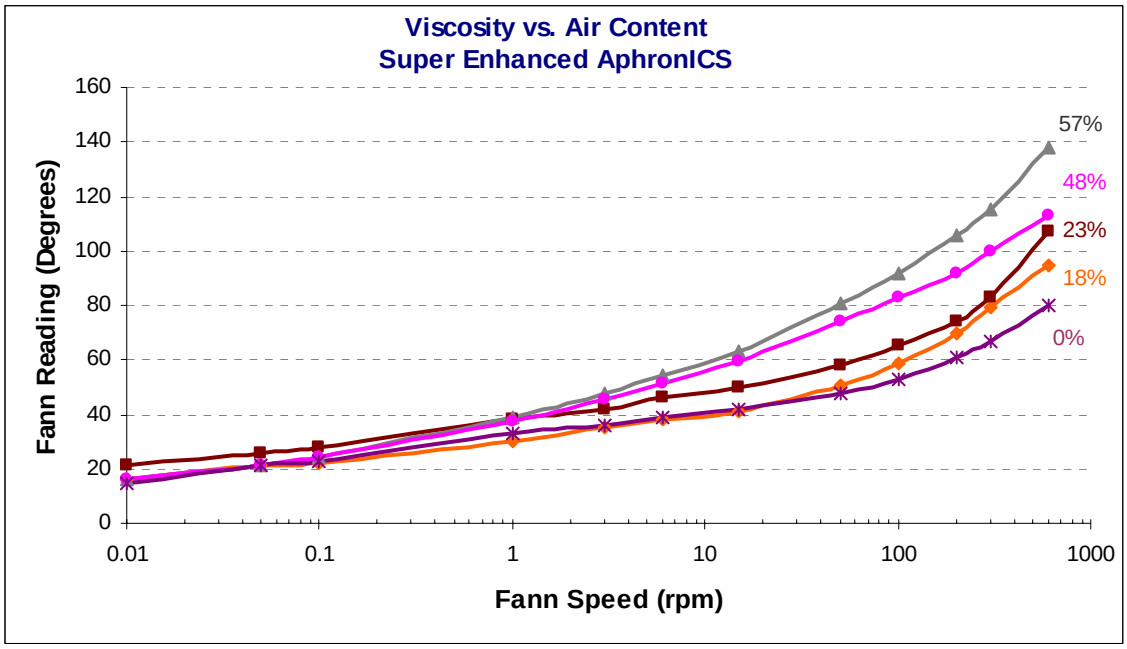

Figure 28. Expanded View of 0.01 to 10 rpm Fann Readings from Figure 27

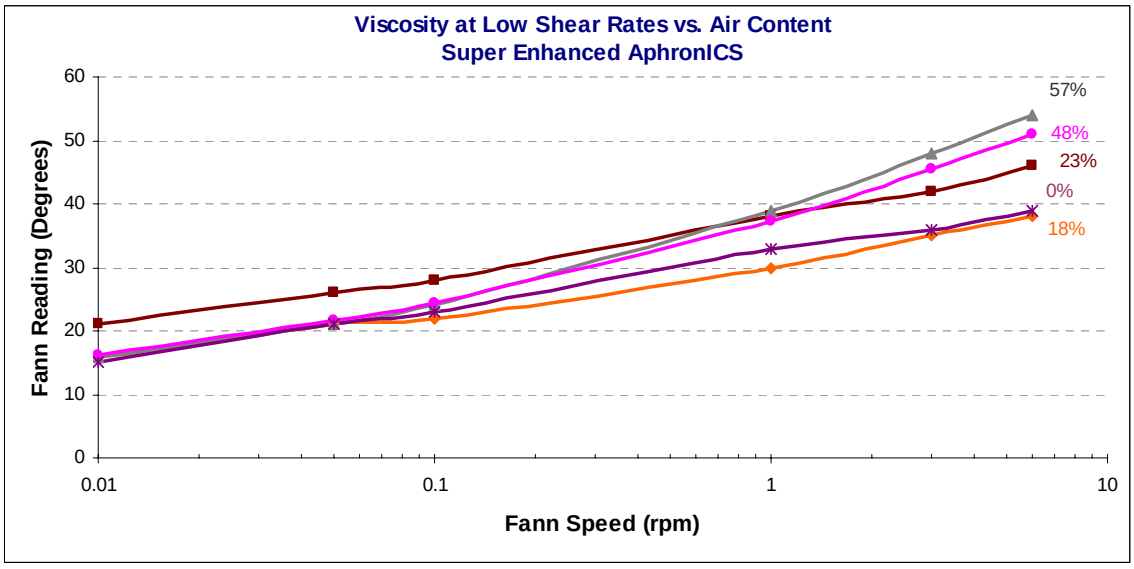

At lower shear rate, the viscosity is less dependent on the concentration of air. The high low-shear-rate viscosity readings of the 23 vol % sample are thought to be in error.

Effect of Temperature on Viscosity:

Figure 29 shows how temperature affects the viscosity of SuperEnhanced APHRON ICS™ fluids over the range 77 to 150 °F.

Figure 29. Effect of Temperature on Viscosity of SE APHRON ICS™ Fluids

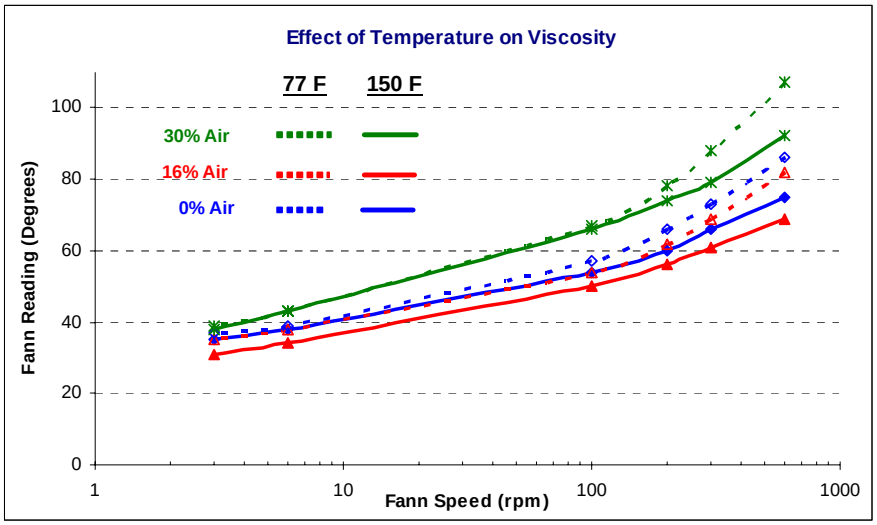

The dashed lines correspond to the rheology profile at room temperature. As expected, viscosity decreases when going up in temperature, though the effect is not very great. Also, in both cases, it can be observed that at higher the air concentration, higher viscosity values are obtained.

Effect of ACTIGUARD on Base Fluid Rheology:

ACTIGUARD is an additive that is an optional component of APHRON ICS™ drilling fluids. It is usually added at a level of 0.5 to 1.0 lb/bbl. ACTIGUARD has some activity as a shale stabilizer, but it is also thought to function as a "mud conditioner," altering the water-wetting/oil-wetting properties of the fluid and the manner in which the other components integrate into the fluid system. However, there is some concern that ACTIGUARD may alter the bulk rheology of the base fluid and the stability of the aphrons.

To address these issues of rheology and aphron stability, deaerated samples of the SuperEnhanced APHRON ICS™ system – one without and one with 1 lb/bbl ACTIGUARD – were prepared, and their viscosity profiles were measured with a Grace M3500 Viscosimeter over the Fann Speed range of 0.01 to 600 rpm. The results are shown in Figures 30 and 31.

Figure 30. Effect of ACTIGUARD on the Rheology of Deaerated SE APHRON ICS™

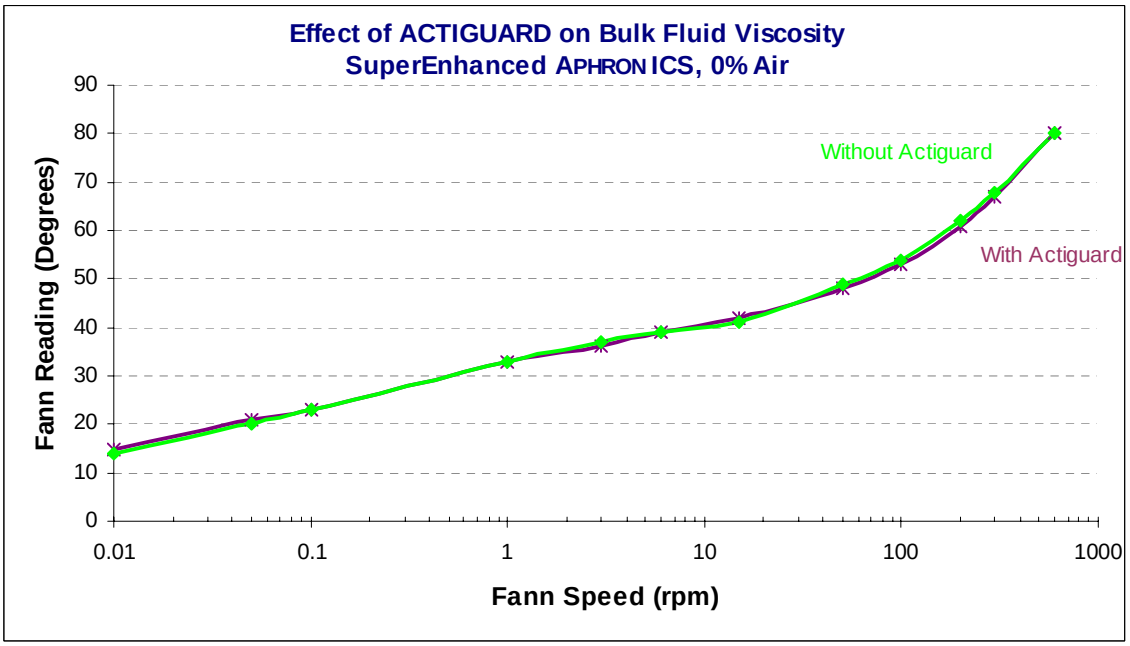

Figure 31. Expanded View of Data at Fann Speeds of 0.01 to 10 rpm from Figure 30

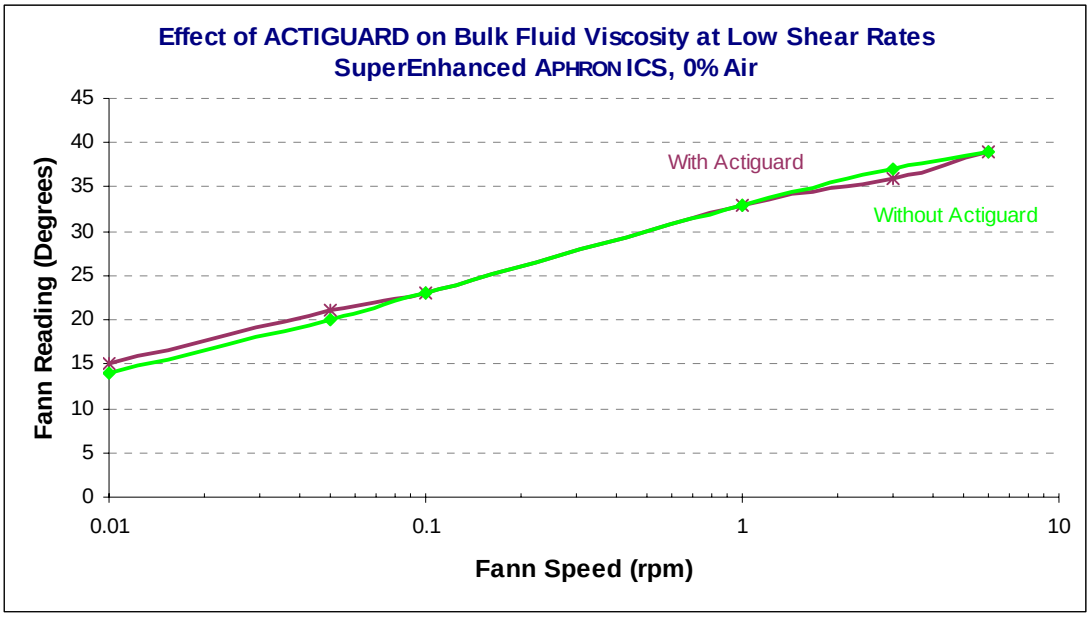

The two plots are basically identical, which indicates that ACTIGUARD has no effect on the rheology of the base fluid.

With regard to the issue of aphron stability, air was entrained in the two samples above using a GE kitchen blender for 1 min, followed by mixing with the Prince Castle mixer (6 min at 9,900 rpm). The sample containing ACTIGUARD had more difficulty entraining air (air content 48% v/v) than the sample without ACTIGUARD (57% v/v), but the half-life of the entrained air appeared to be only slightly lower.

Extensional viscosity will be investigated during the following months. Thus far, only shear viscosity has been considered important for transport of drilling fluids in pipe or in porous media. It has been speculated that extensional viscosity plays a role in the transport of APHRON ICS^{TM} fluids through porous media. Ross Clark of Kelco Rotary (San Diego, CA) has agreed to measure extensional viscosity profiles of several aphron drilling fluids. If extensional viscosity proves to be important, it will be included in the Flow Model being developed at Texas A&M University (see below).

Multi-Phase Flow Effects[8]

For a typical aphron drilling fluid, aphrons are present at such a low concentration that they have a negligible effect on fluid rheology in the wellbore. The fluid is highly shear-thinning and roughly follows a Power Law model even down to a shear rate as low as 0.01 sec^{-1}. At the same time, steady-state values of shear stress are reached within seconds after changing shear rate; thus, the aphron drilling fluids exhibit very low thixotropy. As shown in Figure 32 and detailed in Table 3, more detailed analysis of steady-state viscosimetry data shows that the Herschel-Bulkley model (also known as the "Yield Power Law" model) fits even better, but the best simple model fits are a Carreau[9] model and a Double Power Law model. Based on these comparisons, the Carreau model with Yield was incorporated into a Flow Model for the drilling fluid in the annulus and permeable zone. The main characteristic of this model is that it predicts a constant viscosity μ_0 at very low shear rate and a constant viscosity μ_∞ at high shear rates. For intermediate values of the shear rate, it exhibits a power-law like, highly nonlinear relationship.

Figure 32. Comparisons of Viscosimetry Data and Several Rheological Models

Ambient Temperature and Pressure

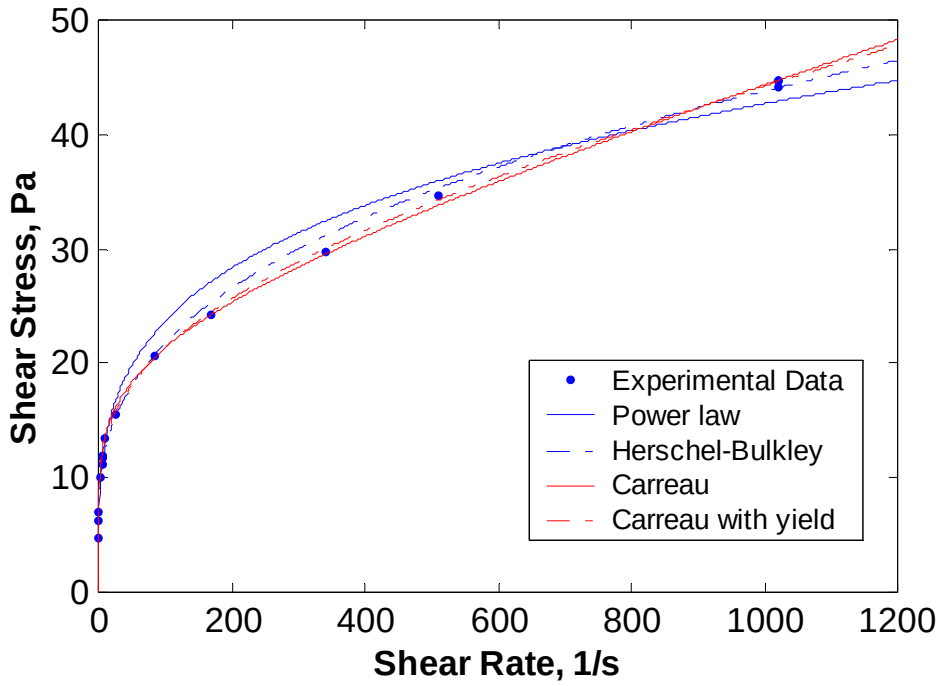

Table 3. Least Squares Residuals for Various Rheological Models

Model	Least-Squares Residual
Power Law – No Yield	**0.0778**
Herschel-Bulkley	**0.0418**
Carreau – No Yield	**0.0291**
Double Power Law	**0.0217**
Carreau – With Yield	**0.0206**

Suppose that an axially symmetric wellbore of radius 0.15 m is drilled in a uniform, isotropic reservoir with 2.5 Darcy permeability. The pressure at the wellbore is 2500 psi (17.3 MPa), and the pressure at a distance of 10 m into the reservoir is 500 psi (3.5 MPa). The equations govern-

ing the flow are Darcy flow through the formation and the conservation of mass. In an annulus, the equation for conservation of mass takes the simple form:

$$\frac{1}{r}\frac{\partial}{\partial r}\left(r\frac{\partial p}{\partial r}\right)=0 \qquad (1)$$

In the fast flow regime, $\mu=\mu_{\infty}=0.0136 Pa\cdot s$; in the slow flow regime, $\mu=\mu_{0}=50.68 Pa\cdot s$. After 24 hours, the aphron fluid has invaded the reservoir to a distance of 10.7 m from the wellbore if the fast flow mode is assumed. If, however, the slow flow mode is assumed, the fluid has invaded only 0.43 m of the reservoir. These two numbers give the bounds in which the invasion of the aphron fluid can happen. The difference is significant, and there is a clear need to establish if and when the regime changes from fast to slow. Note that this drastic change in the invasion depth is only due to a change in the viscosity of the fluid from high to low shear rates.

Simulations using a base fluid with aphrons shows that in the presence of a pressure gradient, a bubble will experience unbalanced forces on its surface and experience "bubbly flow." As a result, it will move relative to the fluid and in the direction of the pressure gradient. The relative velocity U_{rel} of a bubble subjected in a pressure gradient can be related to the Stokes Equation,[9] which is often invoked for gravity-driven settling of weighting material or separation of bubbles. Bubbly flow is proportional to the pressure gradient (∇P), inversely proportional to the fluid viscosity (μ) and proportional to the square of the bubble radius *R*:

$$U_{rel}=\frac{2}{9}\frac{R^{2}}{\mu}\nabla p \qquad (2)$$

In permeable rock under downhole conditions, accumulation of aphrons at the fluid front can create a barrier to flow of liquid or increase the viscosity of the fluid. In either case, increasing the concentration of aphrons slows invasion of the fluid. In modeling this, a constant concentration of about 0.15 vol % of the bubbles was assumed at the wellbore. As the bubbles are released for the first time at the wellbore, they form a front, which starts moving away from the wellbore. Their velocity is a sum of both the fluid velocity and their relative velocity (2) with respect to the fluid. Since at different distances from the wellbore the fluid velocity and pressure gradients are different, the bubbles change speed, generally slowing down as they move away. Furthermore, as

the pressure decreases, they expand and increase the volumetric concentration of gas. To simulate this, the volumetric bubble concentration was computed using a first-order upwind finite difference scheme for bubbles with initial radius 100 μm at several instances of time. The bubble concentration away from the wellbore increases very slowly. However, the bubble profile travels away from the wellbore very quickly, with a speed on the order of meters per second, as shown in Figure 33. This high speed appears to be due to the large pressure gradient, which is of about 10^7 Pa/m near the wellbore. Consequently, as soon as fluid penetrates the permeable rock, bubbles move to the fluid front and concentrate there to form a soft seal.

Since the volume ratio of liquid/air entering the reservoir is constant with time, the thickness of this highly concentrated bubble layer relative to the fluid invasion depth is also nearly constant. For an invasion depth of 10 m, the bubble layer has a thickness of 2-10 cm, depending on the concentration of bubbles in the layer. This bubble layer serves as a barrier to flow of the liquid and effectively slows the rate of invasion of drilling fluid.

Figure 33. Volumetric Bubble Concentration after Release of Aphrons at the Wellbore

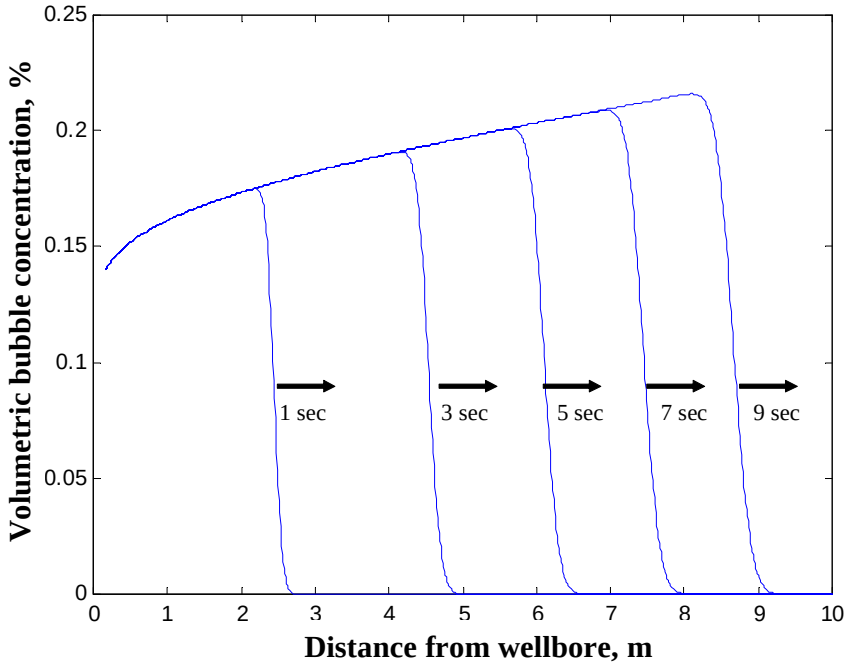

Validation of the model will be attempted this next Quarter with some simple fluid invasion tests. Effects of rock pore geometry, air concentration, BSD, bubble stability, temperature and extensional viscosity may be incorporated into the model later in the year.

6.0 Formation Invasion and Damage Potential

Static Leak-Off Tests

The Aloxite cores included FAO-00, FAO-5, FAO-10 and FAO-40 with nominal air permeability of 2, 5, 10 and 80 Darcy, respectively. The composition of the two "Solids-Free" mud samples is given in Table 4. In addition, the APHRON ICS™ mud contained 17 to 20% air, which was dispersed in the fluid with a Silverson L4RT mixer at 7,000 rpm for 6 min. Both fluids were also treated with 30 lb/bbl $CaCO_3$ of nominal diameter 40 μm; particle size analysis of the sample actually used showed it to possess D_{10} = 0.8 μm, D_{50} = 9 μm and D_{90} = 114 μm. Initially the APHRON ICS™ fluids were all prepared with fresh water, while the FLOPRO NT™ fluids were prepared with 10% NaCl; these are common diluents used in field formulations of the two muds. However, for a fair test of the two fluids, it was determined to prepare both muds using both diluents and perform Leak-Off tests on as many samples as time permitted.

Table 4. Composition of APHRON ICS™ and FLOPRO NT™ Samples*

APHRON ICS™	
Component	**Concentration (lb/bbl)**
Water or 10% NaCl	337 mL
Soda Ash	3.0
X-CIDE	0.1
ACTIVATOR II	2.0
GO-DEVIL II	5.0
ACTIVATOR I	5.0
ACTIGUARD	0.5
BLUE STREAK	1.0
APHRONIZER A	0.5
APHRONIZER B	0.5
PLASTISIZER	0.3

FLOPRO NT™	
Component	**Concentration (lb/bbl)**
Water or 10% NaCl	316 mL
FLO-VIS PLUS	2.3
FLO-TROL	4.5

*For the $CaCO_3$-treated mud samples, the volume of Water or 10% NaCl is reduced by 14 mL.

Some bulk rheological properties of the four fluids are shown in Table 5. The FLOPRO NT™ system is usually run with a LSRV (Low Shear Rate Viscosity) at ambient conditions of 20,000 to 40,000 cP. For these tests, it was determined to optimize the fluid viscosity of the FLOPRO NT™ system so as to compete well with the APHRON ICS™ mud. Consequently, the viscosifier concentration was raised to the maximum level provided in the engineering guidelines, which elevated the LSRV of the brine-based FLOPRO NT™ system to ~ 110,000 cP.

The effects of Back-Pressure and core permeability on Leak-Off were determined first with the "Solids-Free" fresh water-based and 10% NaCl-based drilling fluids. A summary of the results obtained with the Solids-Free fresh-water-based fluids is given in Table 6.

Net Leak-Off is obtained after 30 minutes by subtracting the Dead Volume of water between the mud and the face of the core at the beginning of each test. Dead Volume was approximately 33 mL in all cases. All of the APHRON ICS™ tests resulted in plugging of the cores and production of clear filtrate. Not so for the FLOPRO NT™ system, which was not able to seal even the core with the lowest permeability (FAO-00).

Table 5. Rheology of APHRON ICS™ and FLOPRO NT™ Drilling Fluids

	Fresh Water			10% NaCl			
Test	**AphronICS**	**AphronICS + $CaCO_3$**	**FloPro NT + $CaCO_3$**	**AphronICS**	**Aphron ICS + CaCO3**	**FloPro NT**	**Flo-Pro NT + CaCO3**
Brookfield LVDV-II+, 3L, 0.06 sec^{-1}, 77 F	158000	173000	148000	198000	210000	111000	126000
Grace 3500, 77 F							
600 rpm	92	118	85	114	148	84	90
300 rpm	77	95	72	94	113	68	70
200 rpm	69	84	65	82	108	60	60
100 rpm	59	71	55	67	89	49	49
6 rpm	50	59	34	40	50	26	42
3 rpm	41	46	32	36	45	24	26
Gel Strength - 10 sec	38	41	30	34	39	22	24
Gel Strength - 10 min	47	46	31	38	42	24	29
Gel Strength - 30 min	51	47	31	39	43	24	30
Grace 3500, 150 F							
600 rpm	73	114	62	83	103	62	67
300 rpm	64	89	56	72	87	52	54
200 rpm	59	85	52	65	77	46	48
100 rpm	53	76	45	56	66	39	40
6 rpm	45	63	25	35	40	21	35
3 rpm	35	47	21	32	36	19	23
Gel Strength - 10 sec	33	39		31	33	18	20
Gel Strength - 10 min	42	42		35	36	21	25
Gel Strength - 30 min	44	42		33	37	21	25

When the fresh water used to prepare the mud samples was replaced with 10% NaCl, Leak-Off of the APHRON ICS™ system was markedly reduced, e.g. for FAO-10 with 1000 psi back-pressure, Leak-Off was 9.3 mL/30 min. Meanwhile, FLOPRO NT™ provided no control at all with fresh water or 10% NaCl as the base fluid. Thus, for the Solids-Free fluids, the APHRON ICS™ drilling fluid system yielded good control of Leak-Off, while the FLOPRO NT™ system did not.

Figure 34 shows the relationship between filtrate volume and the square root of time for the Solids-Free fresh water-based APHRON ICS™ and FLOPRO NT™ fluids. This type of graph is used for evaluation of the filtration rate of a drilling fluid after creation of a filter cake.[10] As shown in Figure 34, even with the lowest permeability core, the experiment with FLOPRO NT™ had to be stopped after 8 minutes, because the fluid reservoir was nearly emptied; indeed, the fluid flowed through the core at the maximum flow rate set for the pump, and the pressure drop on the core fell significantly below the pre-set level of 1000 psig.

Both drilling fluids generated similar slopes during the spurt loss phase, as would be expected for fluids possessing similar rheological characteristics. However, the APHRON ICS™ plot bends after 20 sec and ultimately produces a linear Leak-Off vs $t^{1/2}$ plot, which is strong evidence for static formation of some type of filter cake. The FLOPRO NT™ curve did not change slope throughout the 8-min period of that test, which is consistent for a system that does not form a filter cake at all.

Figure 35 shows the Gross Leak-Off obtained with the fresh water-based APHRON ICS™ mud in FAO-5 cores at the three designated Back-Pressures. The results are quite similar and suggest little effect of Back-Pressure, at least in the range 500 to 1500 psig. This is to be expected for incompressible fluids or fluids with a low concentration of a compressible phase. Only when the Back-Pressure was reduced to 0 psig (not shown here) was some effect noted. Note: Here Back-Pressure is reported as Pressure Drop, i.e. Fore-Pressure – Back-Pressure.

Table 6. Net Leak-Off of Solids-Free APHRON ICS™ and FLOPRO NT™ Drilling Fluids

Base Fluid: Fresh Water

Sample	Core	Nominal Gas Permeability, (Darcy)	Mean Pore Diameter, (μm)	Axial Pressure Drop (psi)	Net Leak-Off after 30 min (mL)
APHRON ICS™	FAO-00	2	10	1000	7.0
APHRON ICS™	FAO-5	5	20	1500	10.2
APHRON ICS™	FAO-5	5	20	1000	11.2
APHRON ICS™	FAO-5	5	20	500	11.9
APHRON ICS™	FAO-10	10	35	1500	36.3
APHRON ICS™	FAO-10	10	35	1000	30.8
APHRON ICS™	FAO-10	10	35	500	29.6
FLOPRO NT™	FAO-00	2	10	1000	380*

* Test stopped after 8 minutes

Although Back-Pressure does not affect Leak-Off significantly, Table 6 makes it clear that permeability affects Leak-Off. Indeed, it appears that Leak-Off is roughly proportional to permeability; this is consistent with Darcy Flow, which is typical for flow of fluids through porous media before establishment of a filter cake.

With incorporation of 30 lb/bbl $CaCO_3$ in the APHRON ICS™ and FLOPRO NT™ formulations, Leak-Off was reduced considerably. Table 7 shows the results obtained with the fresh water-based drilling fluids.

Figure 34. Leak-Off vs Time$^{1/2}$ for Solids-Free APHRON ICS™ and FLOPRO NT™

Base Fluid: Fresh Water

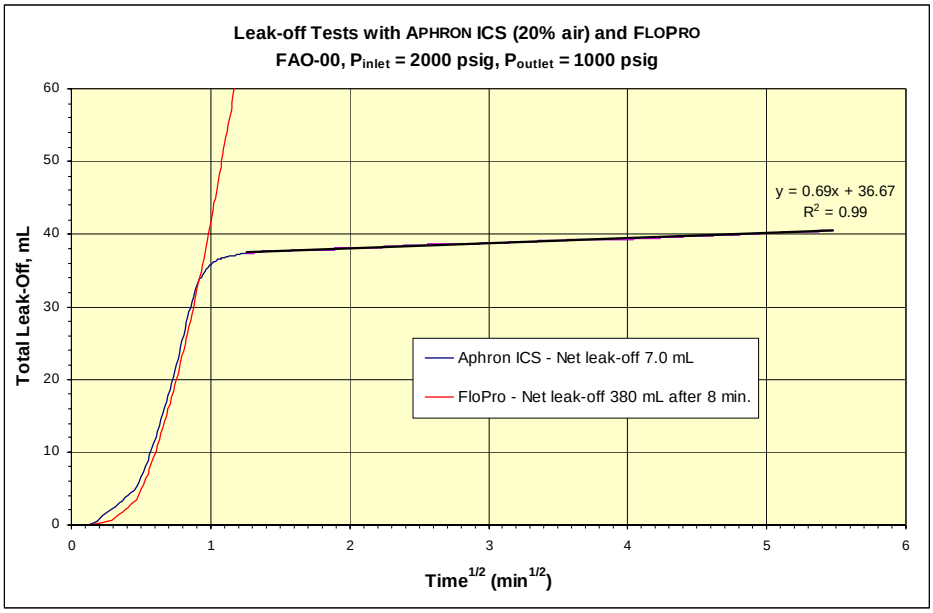

Figure 35. Effect of Back-Pressure on Leak-Off of Solids-Free APHRON ICS™ Mud

Base Fluid: Fresh Water

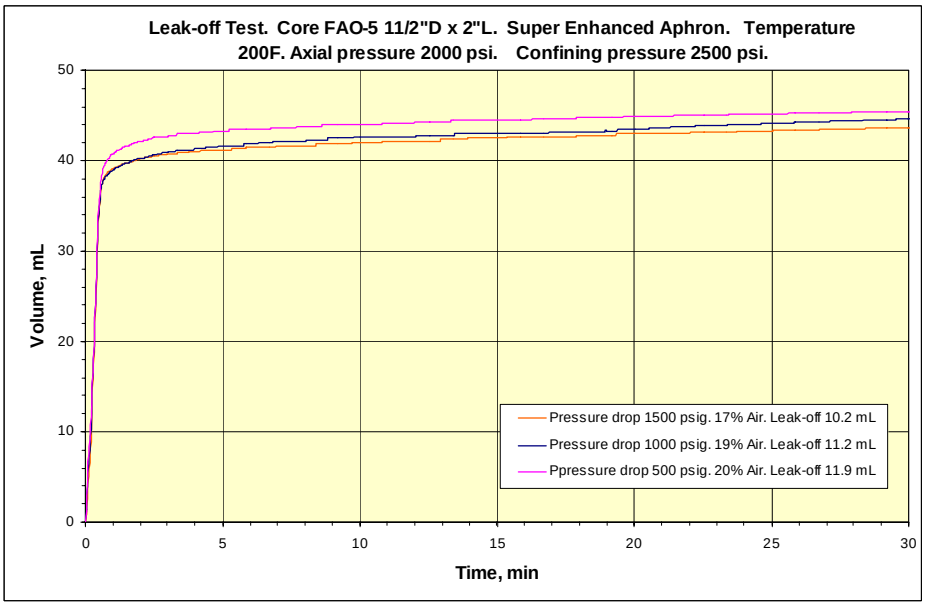

Table 7. Net Leak-Off of $CaCO_3$-Laden APHRON ICS™ and FLOPRO NT™

Base Fluid: Fresh Water

Sample	Core	Nominal Gas Permeability (Darcy)	Mean Pore Diameter (μm)	Axial Pressure Drop (psi)	Net Leak-Off after 30 min (mL)
APHRON ICS™ + 30ppb $CaCO_3$	FAO-5	5	20	1000	8.1
APHRON ICS™ + 30ppb $CaCO_3$	FAO-10	10	35	1000	8.4
APHRON ICS™ + 30ppb $CaCO_3$	FAO-40	80	80	1000	8.0
FLOPRO NT™ + 30ppb $CaCO_3$	FAO-10	10	35	1000	2.9

It is clear that $CaCO_3$ lowered the Leak-Off of both fluids significantly, but it lowered the Leak-Off of the FLOPRO NT™ more, producing a Net Leak-Off of the $CaCO_3$-treated FLOPRO NT™ fluid that was consistently lower than that of the $CaCO_3$-treated APHRON ICS™ fluid. [Note: the Leak-Off curves show the Total Leak-Off, before correcting for the Dead Volume].

Comparison of Figures 36 and 37 shows that the fresh water-based APHRON ICS™ system yields both higher spurt lost and higher filtration rate than fresh water-based FLOPRO NT™. Filter cake formed from APHRON ICS™ + $CaCO_3$ appears to be somewhat thicker and gelatinous compared to that formed from FLOPRO NT™ + $CaCO_3$. Indeed, particle size analysis suggests that the $CaCO_3$ possesses an erodible coating that may affect the manner in which it bridges on the surface of the core.

In 10% NaCl, on the other hand, the $CaCO_3$-laden APHRON ICS™ test results look quite different. As shown in Table 8, the two brine-based drilling fluids produce essentially identical Leak-Offs, within experimental error. This Leak-Off value is independent of permeability and is about the same as that observed for FLOPRO NT™ in fresh water. In this case, all of the filter cakes appeared compact and relatively hard, and the APHRON ICS™ formulation generated a particle size distribution that was similar to that of uncoated $CaCO_3$.

Figure 36. Leak-Off of APHRON ICS™ + 30 lb/bbl $CaCO_3$ in Fresh Water

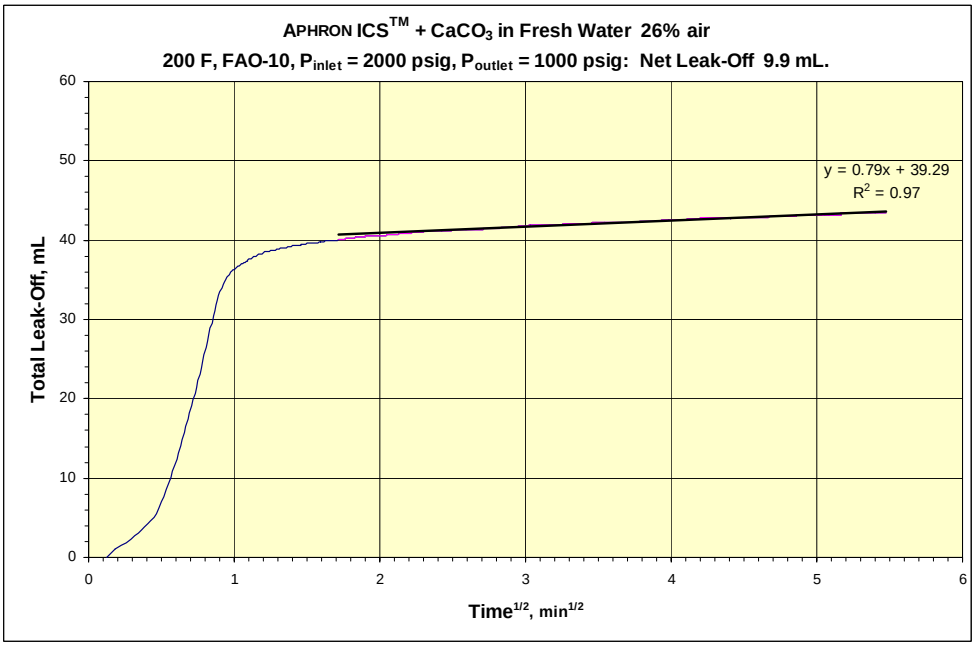

Figure 37. Leak-Off of FLOPRO NT™ + 30 lb/bbl $CaCO_3$ in Fresh Water

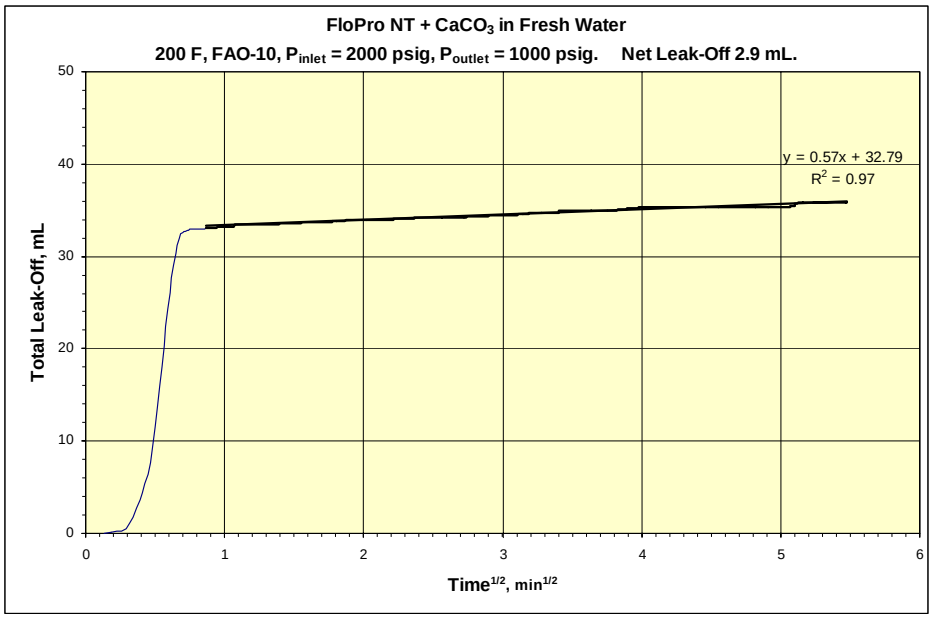

Table 8. Net Leak-Off of $CaCO_3$-Laden APHRON ICS™ and FLOPRO NT™

Base Fluid: 10% NaCl

Sample	Core	Nominal Gas Permeability (Darcy)	Mean Pore Diameter (μm)	Axial Pressure Drop (psi)	Net Leak-Off after 30 min (mL)
APHRON ICS™ + 30ppb $CaCO_3$	FAO-5	5	20	1000	3.2
APHRON ICS™ + 30ppb $CaCO_3$	FAO-10	10	35	1000	3.2
APHRON ICS™ + 30ppb $CaCO_3$	FAO-40	80	80	1000	2.9
FLOPRO NT™ + 30ppb $CaCO_3$	FAO-5	5	20	1000	2.1
FLOPRO NT™ + 30ppb $CaCO_3$	FAO-10	10	35	1000	1.7
FLOPRO NT™ + 30ppb $CaCO_3$	FAO-40	80	80	1000	3.3

Figure 38. Leak-Off of APHRON ICS™ + 30 lb/bbl $CaCO_3$ in 10% NaCl

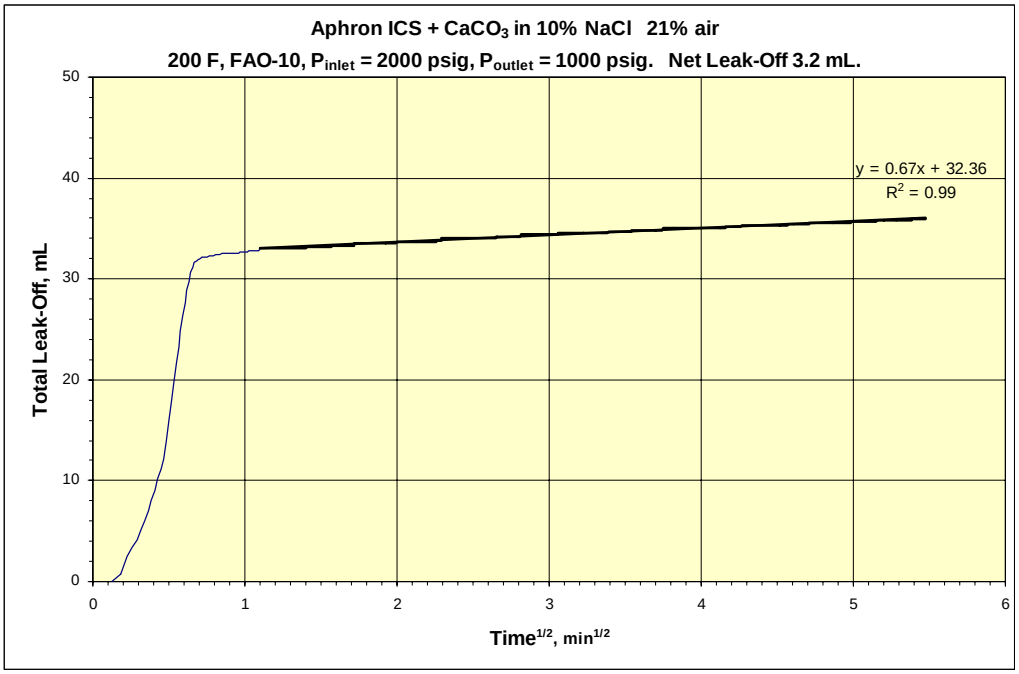

Figure 38 shows the Leak-Off curve obtained for the $CaCO_3$-laden APHRON ICS™ system in 10% NaCl. The shape of the spurt loss phase of the curve is essentially the same as that observed for the $CaCO_3$-laden FLOPRO NT™ system in either fluid medium. The filtration rate, given by the slope of the linear part of the plot (linear with respect to $t^{1/2}$) is only a little higher than that obtained with the FLOPRO NT™ system.

Thus, the Solids-Free APHRON ICS™ system is able to control Leak-Off in these permeable cores relatively well, which is in keeping with its intended application as a Solids-Free drilling fluid. The FLOPRO NT™ system cannot control Leak-Off without the addition of $CaCO_3$. When treated with $CaCO_3$, the FLOPRO NT™ system can control Leak-Off very well, though the brine-based APHRON ICS™ system can match its performance.

Capillary Tube Flow Tests

The determine the effects of the solid components in the APHRON ICS™ system on Leak-Off, four APHRON ICS™ test fluids were prepared from actual chemical components rather than branded products. Composition of the fluids is shown in Table 9, and the rheological properties of Samples #2 - #4 at room temperature are given in Table10.

The results of the capillary flow experiments are shown in Figures 39 and 40; water serves as a reference fluid.

Sample 1, which is not shown, plugged the 0.01 in ID tubing after an essentially negligible amount of fluid was pumped through the tubing. This shows that the FL/CA (Fluid Loss/Conditioning Agent) in that fluid is of sufficient size and quantity to bridge an opening of 0.01 in. The PSD (Particle Size Distribution) of FL/CA in a solution similar to that of an APHRON ICS™ mud shows it to have a very broad range of effective spherical particle size: D_{10} = 1 μm (0.00004 in), D_{50} = 20 μm (0.0008 in) and D_{90} = 103 μm (0.004 in).

Sample 4 contains ACA (Alkalinity Control Agent), instead of FL/CA. ACA has a much narrower PSD that is skewed to lower values: D_{10} = 2 μm (0.00008 in), D_{50} = 10 μm (0.0004 in) and D_{90} = 38 μm (0.0015 in). Having a smaller effective particle size, the ACA passed through the 0.01 in ID tubing, yet it was able to plug the 0.005-in ID tubing.

Table 9. Composition of APHRON ICS™ Test Fluids*

Component	Sample 1	Sample 2	Sample 3	Sample 4
Water	339.	342.	340.	340.
Soda Ash	3.00	3.00	3.00	3.00
Fluid Loss/Conditioning Agent	5.15			
Fluid Loss Agent	1.00	1.00	1.00	1.00
Viscosifying Polymer	3.50	3.50	5.00	3.50
BLUE STREAK	1.00	1.00	1.00	1.00
APHRONIZER A	0.50	0.50	0.50	0.50
APHRONIZER B	0.50	0.50	0.50	0.50
PLASTISIZER	0.30	0.30	0.30	0.30
ACTIGUARD	0.50	0.50	0.50	0.50
Alkalinity Control Agent				2.35

- Concentrations are in lb/bbl

Samples 2 and 3, neither one of which contains particulates (FL/CA or ACA), did not plug either of the capillary tubes. Indeed, the Pressure vs Flow Rate curves appear to correlate with the fluid viscosity, as expected, and with the amount of Viscosifying Polymer. Sample 4, which is identical in composition to Sample 2 save for the ACA, generates a higher Pressure at any Flow Rate, indicating that solids like ACA not only can serve as plugging agents in a sufficiently small orifice, but they also raise the viscosity of the base fluid.

Table 10. Rheology of Test Fluids

Test	Sample 2	Sample 3	Sample 4
Brookfield LVDV-II+, 3L Spindle, 0.06 sec^{-1}, 70 ^{o}F	100000 cP	208000 cP	132000 cP
Grace M3500, 70 ^{o}F			
600 rpm	68	102	82
300 rpm	58	90	69
200 rpm	54	83	62
100 rpm	47	74	53
6 rpm	30	52	35
3 rpm	27	48	33
Gel Strength -10 sec	27	48	32
Gel Strength – 10 min	30	51	34
Gel Strength – 30 min	30	52	35

Figure 39. Pressure vs. Flow Rate in 0.01-in ID Tubing

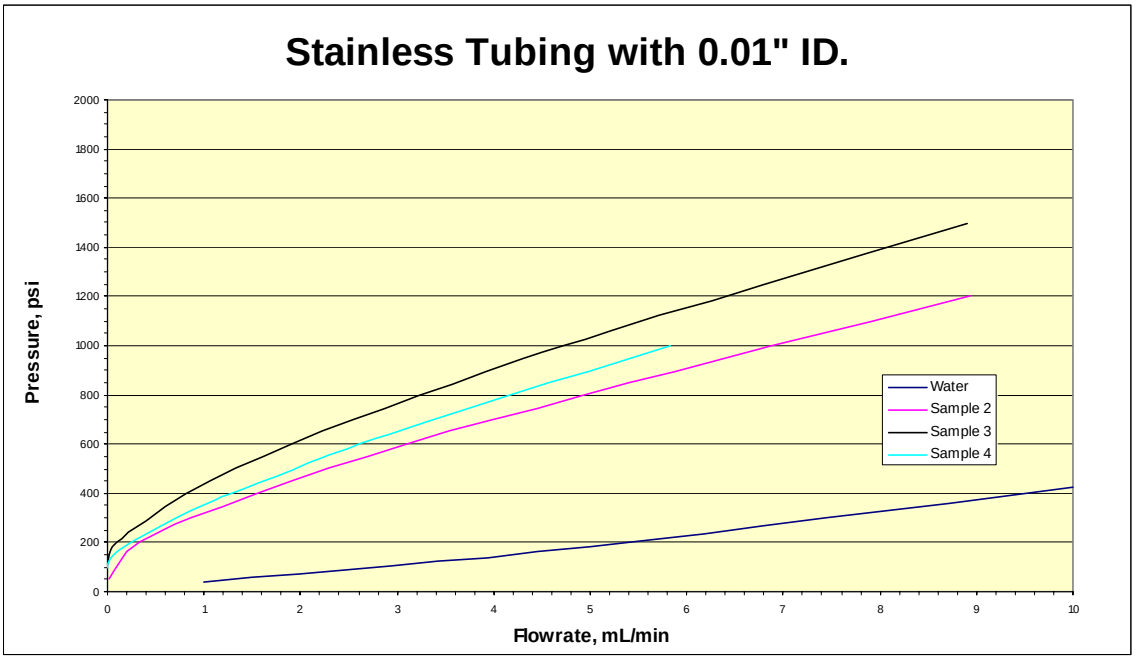

Figure 40. Pressure vs. Flow Rate in 0.005-in ID Tubing

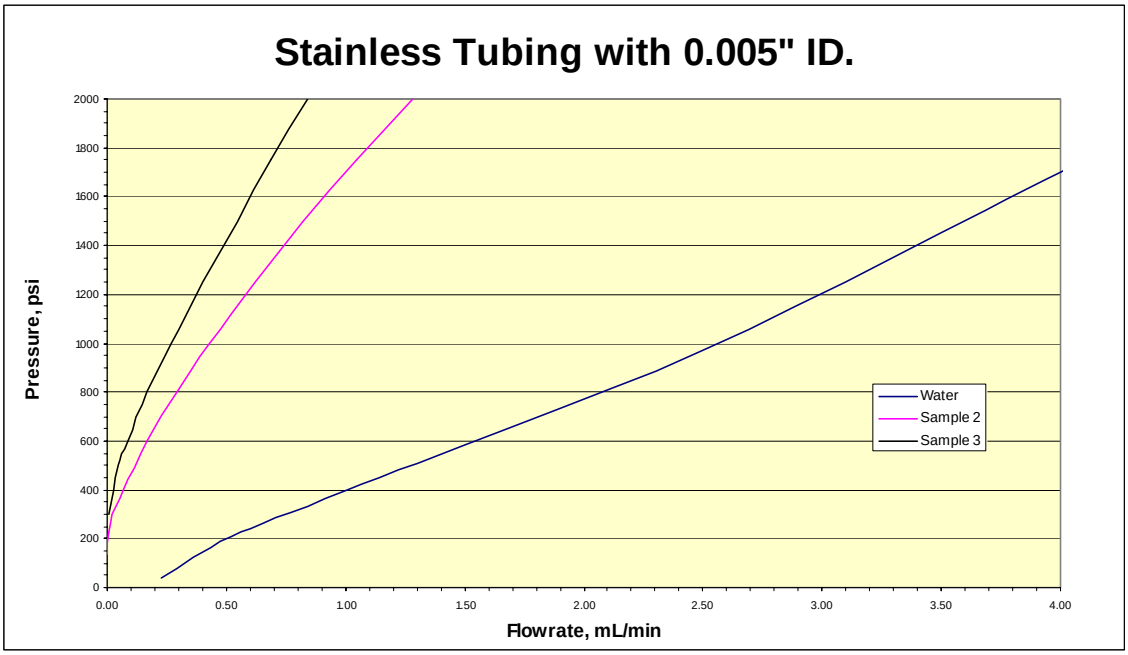

To better understand the roles that air and surfactants play in the invasion control of whole mud and filtrate into permeable media, samples of the SE APHRON ICS™ system were prepared containing (a) the standard complement of surfactants and air, (b) the standard complement of surfactants and no air and (c) no surfactants or air. The composition of the two mud samples (one with and one without surfactants) is given in Table 11. Three types of mud invasion tests were performed to better understand the roles played by the surfactants and air: Modified Capillary Suction Time, Core Leak-Off and Capillary Flow.

After preparation, both samples were hot rolled 16 hours at 150 °F. Because the stability of air bubbles in the fluid without surfactants was much lower than in the standard fluid, the former lost all of its entrained air during heat aging. To compare the base characteristics of these fluids and exclude any effects from aphrons, both samples were deaerated by centrifugation. As made clear by the results in Table 12, the surfactants had a negligible effect on the rheological profile of the SE APHRON ICS™ system. When air (aphrons) was added to the full SE APHRON ICS™ system, it, too, appeared to have no significant effect on the rheology.

Table 11. Composition of SE APHRON ICS™ with and without Surfactants

Component (lb/bbl)	SE APHRON ICS™	SE APHRON ICS™ w/o surfactants
Water	337.0	339.0
Soda Ash	3.0	3.0
ACTIVATOR II	2.0	2.0
GO DEVIL II	5.0	5.0
ACTIVATOR I	5.0	5.0
ACTIGUARD	0.5	0.5
BLUE STREAK	1.0	
APHRONIZER A	0.5	
APHRONIZER B	0.5	0.5
PLASTICISER	0.3	0.3

Table 12. Rheology of SE APHRON ICS™ and SE APHRON ICS™ without Surfactants

	SE APHRON ICS™	SE APHRON ICS™ w/o surfactants
Brookfield LVDV-II+, 3L Spindle, 0.06 sec^{-1}, 70 ^oF	193000	193000
Grace M3500, 70 ^oF		
600 rpm	93	90
300 rpm	78	75
200 rpm	69	67
100 rpm	59	57
6 rpm	39	39
3 rpm	36	36
Gel Strength – 10 sec	36	35
Gel Strength – 10 min	38	37
Gel Strength – 30 min	38	38

On the other hand, both surfactants and air appeared to have a strong effect on filtration rate of the fluid. The Modified Capillary Suction Time test was run on all three fluids; this test generates a Capillary Suction Distance, or CSD, which is a measure of the filtration rate of the fluid. As shown in Table 13, CSD increased upon removal of air from the SE APHRON ICS™ drilling fluid, and it increased further when the surfactants in the drilling fluid were omitted. It is clear that the surfactants, as well as the aphrons, reduce the filtration rate. What is not clear is why the surfactants should play such a strong role. The surface tensions of the full SE APHRON ICS™ fluid and of the SE APHRON ICS™ fluid without BLUE STREAK and APHRONIZER A were determined with a Du Nouy tensiometer to be 34 dyn/cm and 63 dyn/cm, respectively. The low surface tension of the full SE APHRON ICS™ fluid is consistent with surfactant concentrations that are high enough to form micelles. These micelles may be of sufficient size to be incorporated into the filter cake and reduce the filtration rate.

Table 13. Modified Capillary Suction Time (CSD) of APHRON ICS™ with and without Air and without Surfactants

	CSD (mm)			
Fluid	**30 min**	**60 min**	**90 min**	**120 min**
SE APHRON ICS™ 16% air	1.5	3.0	4	4.5
SE APHRON ICS™ 0% air	2.5	4	5.5	7
SE APHRON ICS™ without surfactants	4	6	8	10

Core Leak-Off tests were carried out with the full SE APHRON ICS™ drilling fluid and the SE APHRON ICS™ fluid without BLUE STREAK and APHRONIZER A. All Core Leak-Off tests were carried out at 200 ^{o}F, 2000 psig fore pressure and 1000 psi pressure drop across the 2-in Aloxite cores, using the apparatus described in the previous Monthly Progress Report. When core permeability was low (FAO-00 and FAO-5), the Leak-Off for fluid with surfactants/air was a little lower, as expected, than the Leak-Off for fluids with no surfactants/no air. For cores of higher permeability (FAO-10), the Leak-Off of fluid with surfactants/air was greater than the

Leak-Off for fluid with no surfactants/no air. The results of the Leak-Off experiments are given in Table 14; replicate tests were run with the FAO-5 and FAO-10 cores. The initial FAO-10 Leak-Off curves are shown in Figure 41.

Table 14. Effect of Core Permeability and Surfactants on Leak-Off of SE APHRON ICS™ 200° F, P_{fore} = 2000 psig, P_{back} = 1000 psig, $P_{confining}$ = 2500 psig

Core	Mean Pore Diameter (μm)	SE APHRON ICS™ w/o Surfactants			SE APHRON ICS™ 13% Air		
		Spurt	Filtration	Total	Spurt	Filtration	Total
FAO-00	10	3.8	4.2	8.0	3.1	3.9	7.0
FAO-5	20	8.8	4.0	12.8	6.0	5.2	11.2
		11.4	5.0	16.4			
FAO-10	35	11.6	5.9	17.5	22.5	3.8	26.3
		13.0	5.2	18.2	32.1	3.1	35.2

It is helpful to divide Total Leak-Off into its two components:

Total Core Leak-Off = Spurt + Filtration

where Spurt is the intial invasion of whole fluid before a filter cake is fully established, and Filtration is the invasion of filtrate after a filter cake is formed.[10] Spurt is obtained by extrapolation of the Filtration portion of the curve back to time = 0, and Filtration is given by the balance of the Leak-Off. As expected, both Filtration and Spurt in the FAO-00 and FAO-5 cores appear to be a little lower for the full APHRON ICS™ system than for the system without surfactants and to increase only a little with increasing core permeability. The same is true for Filtration in the FAO-10 core. The Spurt in the FAO-10 core, on the other hand, is anomalously high for the full APHRON ICS™ system.

Figure 41. Effect of Surfactants on Leak-Off vs Time$^{1/2}$ of APHRON ICS^{TM} Drilling Fluids

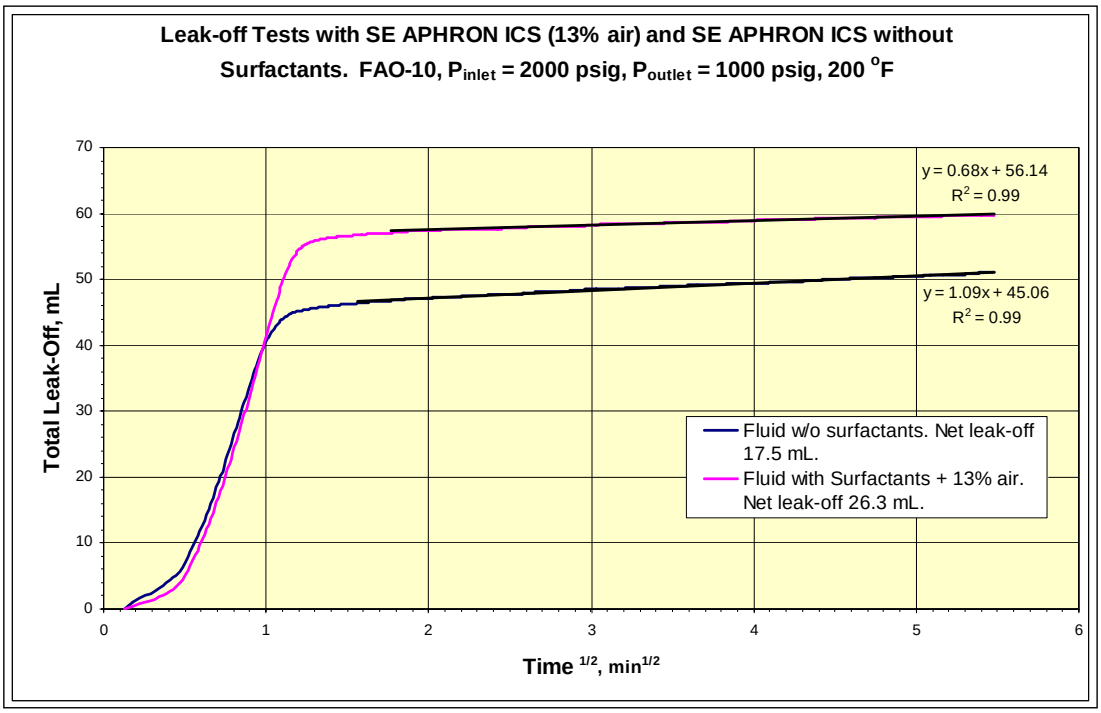

Results of the Capillary Flow experiments with the two fluids are shown in Figures 42 and 43.

In both sizes of tubing, resistance to flow was a little higher for the fluid without surfactants than for the fluids with surfactants. All of the fluids had similar viscosity profiles (see Table 10). One explanation for the slight difference in the Capillary Flow curves is the difference in time required to establish steady-state pressures at any given flow rate. Upon incrementing the flow rate, the pressure generated by the fluid without surfactants reached a steady state value very quickly, whereas the pressure generated by both fluids with surfactants took a long time to stabilize and may not have actually reached a constant (steady state) value. We do not have a reasonable explanation for that temporal behavior but the result is that the reported pressure readings for the fluids with surfactants may have been a little low.

Figure 42. Pressure vs. Flow Rate in 0.02-in (0.5-mm) ID Tubing

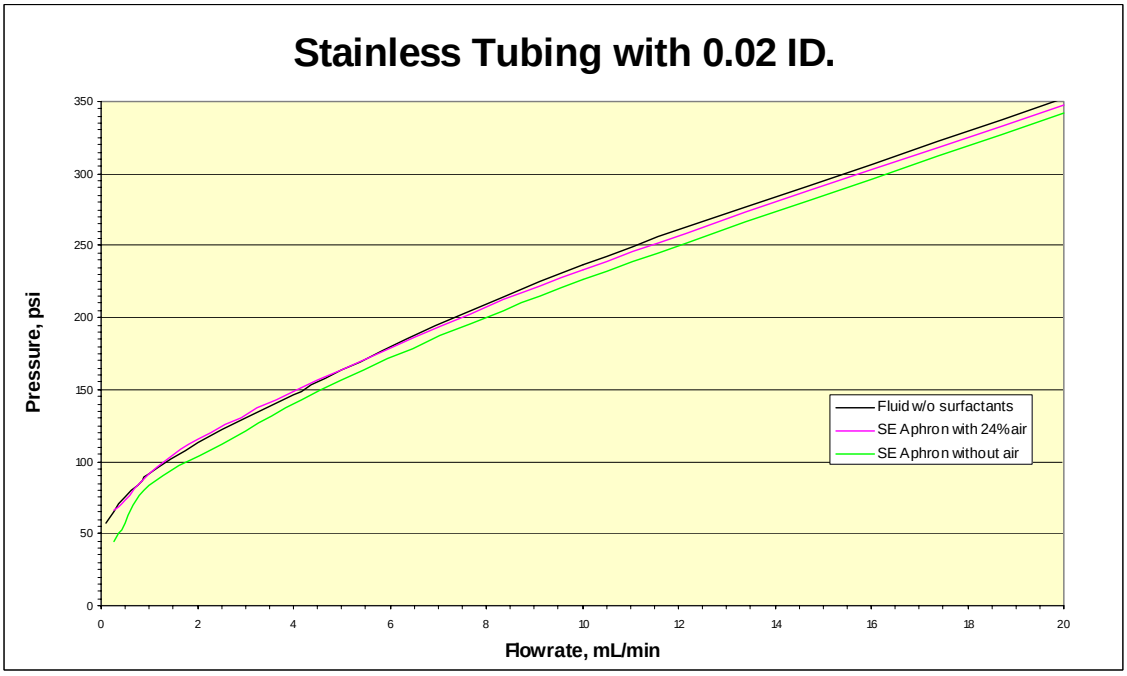

Figure 43. Pressure vs. Flow Rate in 0.03-in (0.76-mm) ID Tubing

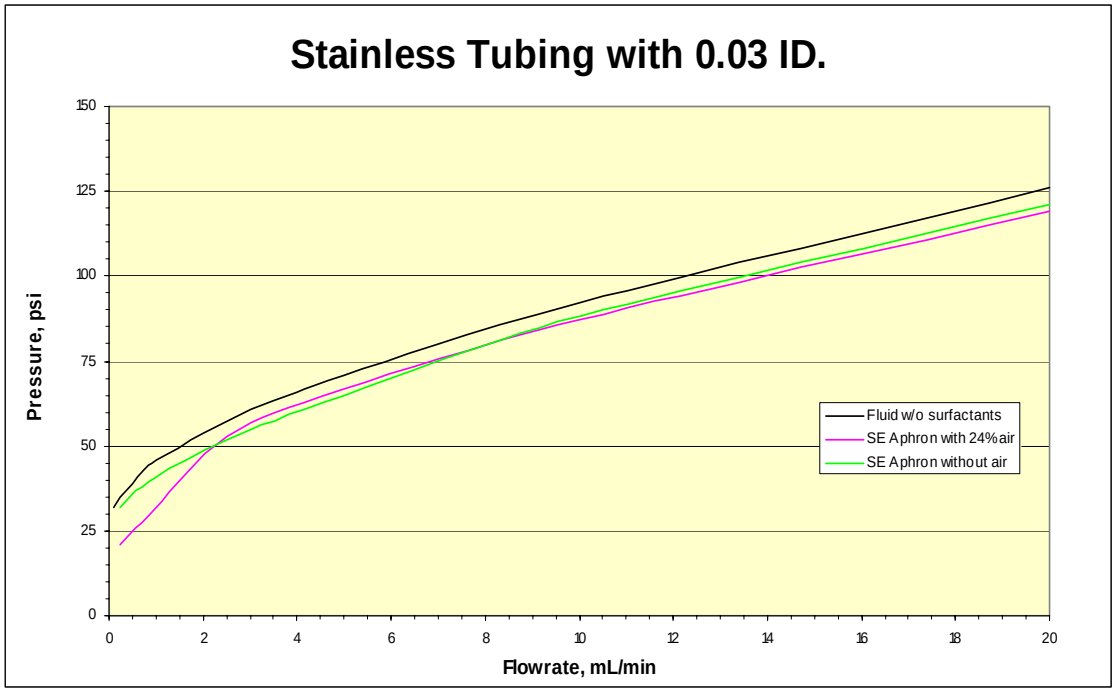

While surfactants in the SE APHRON ICS™ formulation serve to stabilize air and other non-polar internal phases, they are not expected to affect processes that are determined by bulk properties of the fluid, e.g. laminar flow, which is controlled by fluid rheology. Indeed, we have noted no effects of surfactants on rheology as measured via flow in large conduits or concentric cylinder viscosimeters. However, the slow rise of the pressure gradient in the Capillary Flow experiments suggests that surfactants affect flow through capillaries and perhaps other vessels with a high Surface Area / Volume ratio. Surfactants do, of course, affect many processes that involve surface or interfacial properties, such as emulsion stability and wettability. It may be argued that the high surface areas of the filtration media used in Core Leak-Off and Capillary Suction may be influenced by surfactants as well. Thus, not only would aphrons be expected to reduce the rates of fluid invasion in all three tests – Capillary Flow, Leak-Off and Capillary Suction – so would the surfactants themselves. The influence of surfactants on Capillary Flow is reminiscent of the thixotropic effects one observes in concentric cylinder viscosimetry of clay and polymer suspensions. Surfactant micelles could play a role in all three types of tests, as might interaction of the surfactants with other components in the drilling fluid.

CONCLUSIONS

In the area of Aphron Drilling Fluid Optimization, tests of 16 variations of the APHRON ICS™ formulation appear to show that reducing the concentration of viscosifier and increasing the concentration of plasticizer produces greater bubble stability. However, other properties, such as fluid invasion, need to be examined before recommending any change to the fluid formulation. Aphron formation via expansion of APHRON ICS™ muds through drill bit nozzles was simulated with some pressure drop tests at elevated pressure through an orifice; unfortunately, no significant quantities of aphrons were observed. Contact angle measurements of APHRON ICS™ mud on glass pre-wetted with a couple of crude oils showed that the mud will spread; the reverse situation, namely crude oil on APHRON ICS™ mud produces a similar result. These tests demonstrate that the APHRON ICS™ mud and crude oils are compatible and the fluids are expected to intermingle and flow together easily.

In the area of Flow Properties, viscosity profiles of APHRON ICS™ muds containing various amounts of air indicate that above 10 to 15 vol % air the viscosity increases at shear rates above 1 rpm (1.6 sec^{-1}), but not below that shear rate. The effect of temperature over the range 76 to 150 ^{o}F is quite modest; only above 100 rpm (160 sec^{-1}) was any reduction in viscosity observed. A fluid invasion model has been developed by Dr. Peter Popov of Texas A&M University, which shows that under downhole conditions the rheology of the APHRON ICS™ fluid can control its depth of invasion to a couple of meters. Aphrons, solids and surfactants may reduce this further, but additional work will need to be carried out to quantify those effects.

Finally, in the area of Formation Invasion and Damage Potential, linear, static Leak-Off tests at 200 ^{o}F, Fore-Pressure = 2000 psig and Back-Pressure = 1000 psig showed that Solids-Free APHRON ICS™ fluid can seal Aloxite cores ranging in permeability from 2 to 10 Darcy; the Leak-Off is commensurate with the permeability of the core. The Solids-Free standard reservoir drilling fluid FLOPRO NT™ drilling fluid, on the other hand, is not able to seal a 2-Darcy core. With addition of 30 ppb $CaCO_3$, both fluids provided similar ultra-low Leak-Off. Capillary Flow tests, along with Core Leak-Off and Modified Capillary Suction tests indicate that the solids and surfactants in APHRON ICS drilling fluids play major roles in reducing fluid invasion in both low- and high-permeability media.

REFERENCES

1. Montilva, J., Ivan, C.D., Friedheim, J. and Bayter, R.: "Aphron Drilling Fluid: Field Lessons From Successful Application in Drilling Depleted Reservoirs in Lake Maracaibo," OTC 14278, presented at the 2002 Offshore Technology Conference, Houston, May 6-9, 2002.
2. Growcock, F.B., Simon, G.A., Rea, A.B., Leonard, R.S., Noello, E. and Castellan, R.: "Alternative Aphron-Based Drilling Fluid," IADC/SPE 87134, presented at the 2004 IADC/SPE Drilling Conference, Dallas, Mar. 2-4, 2004.
3. Brookey, T., Rea, A. and Roe, T.: "UBD and Beyond: Aphron Drilling Fluids for Depleted Zones," presented at IADC World Drilling Conference, Vienna, Austria, Jun. 25-26, 2003.
4. Growcock, F.B., Simon, G.A., Guzman, J., and Paiuk, B.: "Applications of Novel Aphron Drilling Fluids," AADE-04-DF-HO-18, presented at the AADE 2004 Drilling Fluids Conference, Houston, TX, Apr. 6-7, 2004.
5. Sebba, F.: **Foams and Biliquid Foams – Aphrons**, John Wiley & Sons Ltd, Chichester (1987).
6. White, C.C., Chesters, A.P., Ivan, C.D., Maikranz, S. and Nouris, R.: "Aphron-Based Drilling Fluid: Novel Technology for Drilling Depleted Formations," World Oil, Vol. 224, No. 10 (Oct. 2003).
7. Walker, J.: "The Amateur Scientist: Fluid Interfaces, Including Fractal Flows Can Be Studied in a Hele-Shaw Cell," Scientific American, No. 257, pp. 134-138, Nov. 1987.
8. Popov, P.: Private Communication, Texas A&M University, March 15, 2005.
9. Landau, L. D. and Lifshitz, E. M.: **Fluid Mechanics (Course of Theoretical Physics, Vol. 6)**, 2nd Edition, Butterworth-Heinemann, 1995.
10. Darley, H. C. H. and Gray, G. R.: Composition and Properties of Drilling and Completion Fluids, Fifth Edition. Gulf Professional Publishing (1988).

LIST OF ACRONYMS AND ABBREVIATIONS

APHRON ICS™ = Polymer-Based Aphron Invasion Control System

BSD = Bubble Size Distribution

D_{50} = Median bubble size, i.e. half of the bubbles are greater than and half are less than the stated value.

HTHP = High Temperature and High Pressure

LSRV = Low Shear Rate Viscosity, generally measured at 0.06 sec^{-1}

ppb = lbm/bbl = Pounds (mass) per Barrel

psia = lbf/in^2 = Absolute Pressure

psig = Gauge Pressure, i.e. psig = psia + 14.7

SE APHRON ICS™ = SuperEnhanced APHRON ICS™